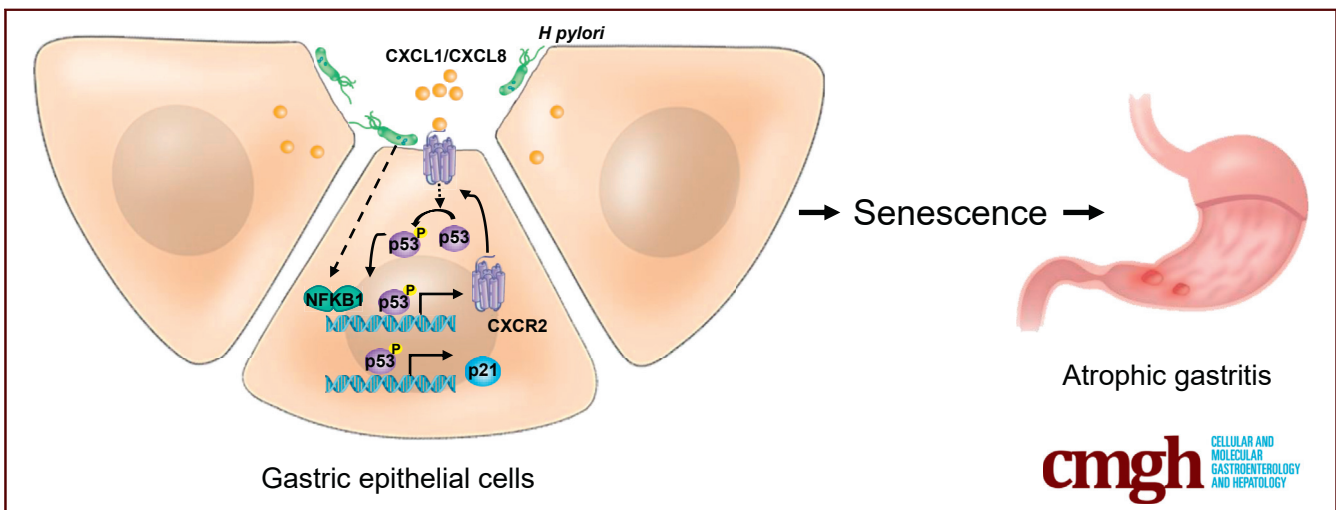


## ORIGINAL RESEARCH

Inflammation-Associated Senescence Promotes *Helicobacter pylori*-Induced Atrophic Gastritis

Qinbo Cai,<sup>1,2,4</sup> Peng Shi,<sup>1,2,4</sup> Yujie Yuan,<sup>1,2</sup> Jianjun Peng,<sup>1,2</sup> Xinde Ou,<sup>1,2,4</sup> Wen Zhou,<sup>1,2,4</sup> Jin Li,<sup>1,2,3,4</sup> Taiqiang Su,<sup>1,2,3,4</sup> Liangliang Lin,<sup>1,2</sup> Shirong Cai,<sup>1,2</sup> Yulong He,<sup>1,2,3</sup> and Jianbo Xu<sup>1,2</sup>

<sup>1</sup>Center of Gastrointestinal Surgery, the First Affiliated Hospital of Sun Yat-sen University, Guangzhou, China, <sup>2</sup>Center for Diagnosis and Treatment of Gastric Cancer, Sun Yat-sen University, Guangdong, China; <sup>3</sup>Center for Digestive Disease, the Seventh Affiliated Hospital of Sun Yat-sen University, Shenzhen, China, <sup>4</sup>Laboratory of General Surgery, the First Affiliated Hospital of Sun Yat-sen University, Guangzhou, China



## SUMMARY

Cellular senescence is a new mechanism for *Helicobacter pylori*-induced atrophic gastritis, and *H. pylori* promotes senescence through inflammatory C-X-C motif chemokine receptor 2 signaling. Inhibition of C-X-C motif chemokine receptor 2 signaling is a potential therapy to prevent atrophic gastritis and subsequent precancerous lesions.

**BACKGROUND & AIMS:** The association between cellular senescence and *Helicobacter pylori*-induced atrophic gastritis is not clear. Here, we explore the role of cellular senescence in *H. pylori*-induced atrophic gastritis and the underlying mechanism.

**METHODS:** C57BL/6J mice were infected with *H. pylori* for biological and mechanistic studies in vivo. Gastric precancerous lesions from patients and mouse models were collected and analyzed using senescence-associated beta-galactosidase, Sudan Black B, and immunohistochemical staining to analyze senescent cells, signaling pathways, and *H. pylori* infection. Chromatin immunoprecipitation, luciferase reporter assays, and other techniques were used to explore the underlying mechanism in vitro.

**RESULTS:** Gastric mucosa atrophy was highly associated with cellular senescence. *H. pylori* promoted gastric epithelial cell senescence in vitro and in vivo in a manner that depended on

C-X-C motif chemokine receptor 2 (CXCR2) signaling. Interestingly, *H. pylori* infection not only up-regulated the expression of CXCR2 ligands, C-X-C motif chemokine ligands 1 and 8, but also transcriptionally up-regulated the expression of CXCR2 via the nuclear factor- $\kappa$ B subunit 1 directly. In addition, CXCR2 formed a positive feedback loop with p53 to continually enhance senescence. Pharmaceutical inhibition of CXCR2 in an *H. pylori*-infected mouse model attenuated mucosal senescence and atrophy, and delayed further precancerous lesion progression.

**CONCLUSIONS:** Our study showed a new mechanism of *H. pylori*-induced atrophic gastritis through CXCR2-mediated cellular senescence. Inhibition of CXCR2 signaling is suggested as a potential preventive therapy for targeting *H. pylori*-induced atrophic gastritis. GEO data set accession numbers: GSE47797 and GSE3556. (*Cell Mol Gastroenterol Hepatol* 2021;11:857–880; <https://doi.org/10.1016/j.jcmgh.2020.10.015>)

**Keywords:** *H. pylori*; Mucosa Atrophy; Senescent Cell; C-X-C Motif Chemokine Receptor 2.

Atrophic gastritis is a pivotal stage in the multistep process of intestinal-type gastric carcinogenesis, which includes the sequential development of chronic gastritis (CG), atrophic gastritis (AG), intestinal metaplasia

(IM), dysplasia (DP), and, finally, gastric cancer.<sup>1,2</sup> AG is a strong risk factor for gastric cancer, and patients with AG have a 3.5-fold increased risk of developing gastric cancer.<sup>3</sup> *Helicobacter pylori* infection is the most important cause of nonautoimmune AG, with a high odds ratio of 6.4.<sup>4,5</sup> Some mechanisms underlying *H pylori*-induced AG have been reported. *H pylori* attachment can cause direct damage to the surface epithelial cells via actin polymerization within the cells. In addition, *H pylori* adhesion induces many inflammatory factors, such as C-X-C motif chemokine ligand 8 (CXCL8), interleukin (IL)1, IL6, and tumor necrosis factor- $\alpha$ . In addition, apoptosis is proposed as a possible mechanism of mucosal epithelial damage under *H pylori* infection.<sup>6–8</sup> However, adhesion-dependent mechanisms are unlikely to function in oxyntic or chief cells because *H pylori* always resides in the vicinity of surface and foveolar mucous cells, but does not reach the oxyntic glands.<sup>9</sup> It seems that inflammation-dependent mechanisms can partly explain damage in oxyntic or chief cells because inflammatory cells and inflammatory cytokines infiltrate the entire gastric mucosa.<sup>10</sup>

Cellular senescence is a specific phenomenon wherein a proliferation-competent cell undergoes permanent growth arrest under various cellular stresses, such as DNA damage and oncogene activation.<sup>11</sup> Cellular senescence is considered one of the most important barriers to tumorigenesis<sup>12</sup> and often is observed in premalignant lesions leading to prostate, lung, or breast cancer. However, the dual role of senescence in tumorigenesis recently was described.<sup>13</sup> Senescent cells express a large number of secreted proteins that result in a specific “senescence-associated secretory phenotype” (SASP), often accompanying these processes.<sup>14</sup> SASP includes inflammatory cytokines and chemokines and leads to the inflammatory response, which can be both beneficial and harmful. For example, SASP can induce immune suppression and promote tumor cell proliferation and invasion.<sup>15–17</sup> *H pylori* infection induces various inflammatory factors, such as CXCL8 and CXCL1, which also have been identified as part of the SASP.<sup>13</sup> In addition, it has been reported that cytotoxin-associated gene A (CagA), the important virulence factor of *H pylori*, can induce cellular senescence via the regulation of p21.<sup>18</sup> These evidences indicate that *H pylori* infection might induce the senescence of gastric epithelial cells. One of the important features of atrophic mucosa is that glands lose the ability to regenerate.<sup>6</sup> If *H pylori* can induce gland cell senescence through adhesion-dependent or independent mechanisms, then cellular senescence could be another mechanism of *H pylori*-induced AG. However, it was reported that senescent cells were detectable in IM and reduced in gastric cancer,<sup>19</sup> but whether senescent cells exist in atrophic mucosa has not been reported. Here, we show that cellular senescence is a new mechanism of *H pylori*-induced AG and that *H pylori* promotes the senescence of gastric epithelial cells via C-X-C motif chemokine receptor 2 (CXCR2) signaling. Pharmaceutical inhibition of CXCR2 attenuated mucosa senescence and atrophy under *H pylori* infection in vivo.

## Results

### Senescent Cells Are Abundant in Atrophic Mucosa

It remains unknown whether cellular senescence is associated with *H pylori*-induced AG. To answer this question, we first collected fresh gastric mucosa biopsy samples from a patient diagnosed with CG, AG, and IM who also was positive for *H pylori* infection. Sometimes AG is accompanied by IM or DP. In this study, AG was defined as pure mucosa atrophy without IM or DP so that we could better understand the mechanism of different stages. By using senescence-associated beta-galactosidase (SA- $\beta$ -gal) staining, we detected abundant senescent cells in mucosal glands with AG, but not in those with CG. In atrophic mucosa in which gastric glands were partly replaced with intestinal glands, a large amount of senescent cells could be detected in the intestinal glands. However, senescent cells hardly raised in intestinal glands located in mucosa with little normal gastric mucosa loss (Figure 1A). It seemed that cellular senescence was highly related to *H pylori*-induced mucosa atrophy. To confirm this hypothesis, we retrospectively collected formalin-fixed gastric mucosa biopsy samples from 20 patients diagnosed with *H pylori*-induced CG combined with AG, IM, and DP at the same time. We used Sudan Black B staining to detect senescent cells in these samples because SA- $\beta$ -gal staining cannot be applied to formalin-fixed samples. The results showed that senescent cells were the most abundant in AG mucosa without IM or DP, followed by mucosa with IM (Figure 1B). We also used a mouse-adapted *H pylori* strain, the pre-mouse Sydney strain 1 (PMSS1), to generate an *H pylori*-infected mouse model (Figure 2D). The abilities of PMSS1, such as activating nuclear factor- $\kappa$ B (NF- $\kappa$ B) signaling and up-regulating CXCL8 messenger RNA (mRNA), were confirmed before infection (Figure 2A–C). We used SA- $\beta$ -gal staining to detect senescent cells in precancerous lesions from this *H pylori*-infected mouse model, and the results were similar to those in the patient samples. Abundant senescent cells were detected in mucosa with pure AG, but not in mucosa with CG, IM, or DP (Figure 2F).

Based on these results, we conclude that senescent cells might be strongly related to *H pylori*-induced AG.

**Abbreviations used in this paper:** AG, atrophic gastritis; BrdU, bromodeoxyuridine; CagA, cytotoxin-associated gene A; CDKN, cyclin-dependent kinase inhibitor; CG, chronic gastritis; ChIP, chromatin immunoprecipitation; CXCL, C-X-C motif chemokine ligand; CXCR2, C-X-C motif chemokine receptor 2; DP, dysplasia; GEO, Gene Expression Omnibus; GSEA, gene set enrichment analysis; IHC, immunohistochemical; IL, interleukin; IM, intestinal metaplasia; MNU, N-methyl-N-nitrosourea; MOI, multiplicity of infection; mRNA, messenger RNA; NF- $\kappa$ B, nuclear factor- $\kappa$ B; NFKB1, nuclear factor- $\kappa$ B subunit 1; PBS, phosphate-buffered saline; PMSS1, pre-mouse Sydney strain 1; qPCR, quantitative polymerase chain reaction; RELA, RELA proto-oncogene, nuclear factor- $\kappa$ B subunit; SASP, senescence-associated secretory phenotype; TP53, tumor protein p53.

 Most current article

© 2020 The Authors. Published by Elsevier Inc. on behalf of the AGA Institute. This is an open access article under the CC BY-NC-ND license (<http://creativecommons.org/licenses/by-nc-nd/4.0/>).

2352-345X

<https://doi.org/10.1016/j.jcmgh.2020.10.015>

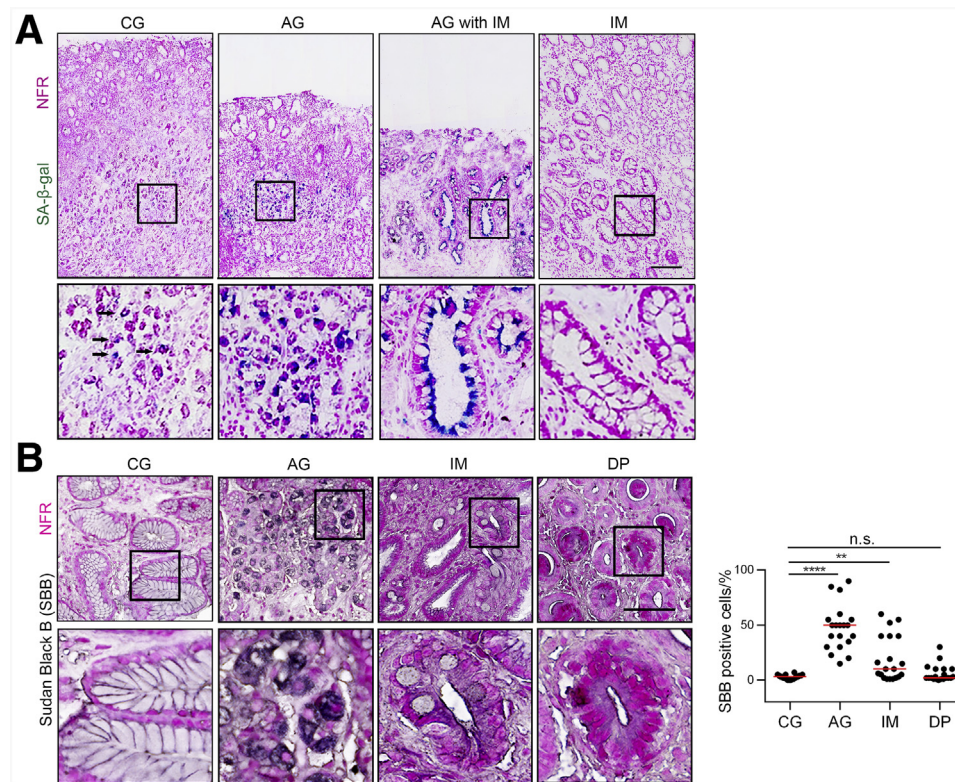


**Figure 1. Cellular senescence is highly associated with *H pylori*-induced atrophic gastritis.** (A) Mucosa images (from antrum) from a representative patient diagnosed with CG, AG, and IM. Senescent cells are stained with SA-β-gal. Scale bar: 200 μm. Black arrows refer to SA-β-gal-positive cells. (B) Senescent cells were detected by Sudan Black B staining in human mucosa biopsy samples (from antrum, 20 patients diagnosed with CG, AG, IM, and DP at the same time). CG was restricted to mucosa without AG, IM, or DP. AG was restricted to atrophic mucosa without IM or DP. IM was restricted to mucosa without DP. Plot: median. Scale bar: 100 μm. Significant differences were analyzed using the Mann-Whitney test. The boxed areas show where the larger image in the down panel come from. \*\* $P < .01$ . \*\*\*\* $P < .0001$ . NFR, nuclear fast red.

### *H pylori* Infection Promotes Senescence in Gastric Mucosal Cells

Because we showed earlier that senescent cells were abundant in *H pylori*-induced AG, we next investigated whether *H pylori* infection could promote senescence in gastric mucosa. We found that senescent cells were easily detected in *H pylori*-colonized mouse mucosa, whereas almost no senescent cells could be detected in mucosa from the *H pylori*-uninfected control mice (Figure 2E). We then investigated whether a positive *H pylori* infection was associated with an increased number of senescent cells in formalin-fixed gastric mucosa biopsy samples from the 20 patients mentioned earlier. Some of these patients had received *H pylori* eradication treatment; thus, possibly, no *H pylori* infection might be detected in some of the samples if there was no re-infection. We used immunohistochemical staining (IHC) to identify *H pylori* infection and divided them into 2 groups (*H pylori*-negative and *H pylori*-positive groups) (Figure 2G), and the results showed that senescent cells were much more abundant in the *H pylori*-positive group (Figure 2H).

Furthermore, we observed that PMSS1 enhanced the senescence of AGS and GES-1 cells in a multiplicity of infection (MOI)-dependent manner in vitro (Figure 2I and J). GES-1 is

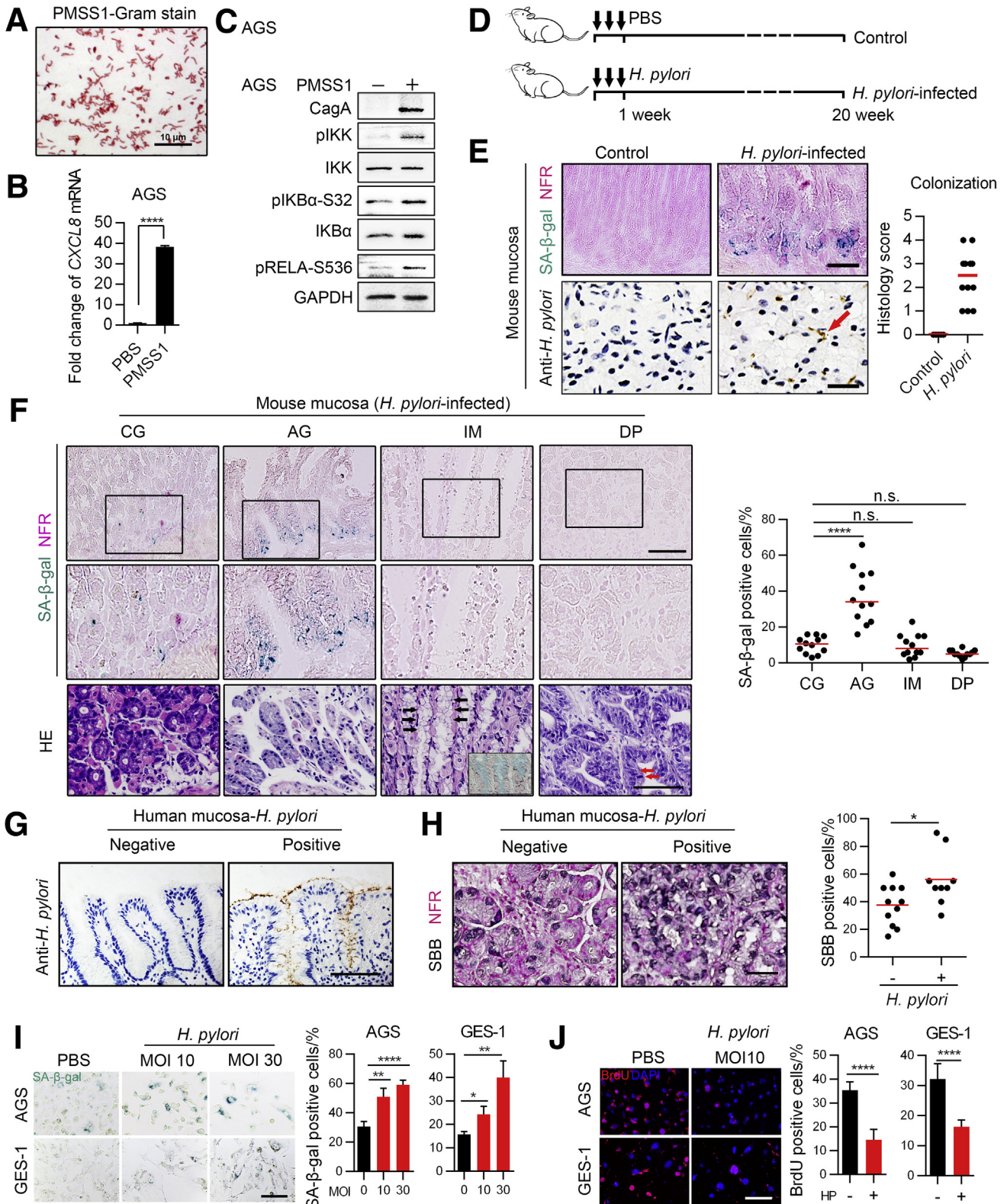
an immortalized gastric epithelial cell line transformed by the SV40 large T-antigen from primary gastric mucosal cells.<sup>20</sup> Thus, according to our results, *H pylori* significantly enhances the senescence of mucosal epithelial cells.

### *H pylori* Promotes Senescence in Gastric Mucosa via CXCR2 Signaling

To explore the pathways involved in *H pylori*-mediated senescence, we used gene set enrichment analysis (GSEA) to analyze expression profiles from Gene Expression Omnibus (GEO) data sets. We found that the CXCL8/CXCR2 pathway had a much higher enrichment score than other senescence-associated gene sets in both *H pylori*-infected human samples (GSE47797) and cell lines (GSE3556) (Figure 3A). CXCR2 is a G-protein-coupled cell surface chemokine receptor; its most important ligands are CXCL8 and CXCL1, but other CXCR2 ligands include CXCL2, CXCL3, CXCL5, CXCL6, and CXCL7.<sup>21</sup> CXCR2 signaling has been reported to promote cellular senescence.<sup>22-24</sup> To confirm that CXCR2 signaling can be activated by *H pylori*, we evaluated the expression of CXCR2 and its most important ligands, CXCL8 and CXCL1, in AGS and GES-1 cells infected with PMSS1 in vitro. *CXCL8* mRNA and *CXCL1* mRNA were both up-regulated as

previously reported.<sup>25</sup> To our surprise, we found that both the mRNA and protein expression of CXCR2 also were up-regulated significantly by *H. pylori* in an MOI-dependent

manner (Figure 3B and C). To further confirm this, we evaluated whether positive *H. pylori* infection was associated with higher expression of CXCR2 in human mucosa from the 20



patients mentioned previously. Overall, positive *H pylori* infection was associated significantly with higher CXCR2 expression in mucosal glands (Figure 3D). Specifically, we found that CXCR2 was expressed most highly in the base of glands in mucosa with AG (Figure 3E). The base of glands contains mainly parietal cells and chief cells, which generally are lost and replaced during AG.<sup>8</sup> In our study, we also observed that senescent cells were most abundant in the base of glands in both human mucosa and mouse mucosa with AG (Figure 1A and 2E, left upper panel). When we assessed CXCR2 expression according to pathologic type, we found that CXCR2 expression was higher in mucosa with AG, IM, or DP than in mucosa with CG (Figure 3F). In mouse mucosa, *H pylori* infection also significantly up-regulated Cxcr2 and Cxcl1 protein levels (Figure 3G and H) and mRNA levels (Figure 3J). The protein level of CXCR2 was correlated positively with the proportion of senescent cells in both human and mouse mucosa with AG (Figure 3J). This evidence strongly supports the hypothesis that *H pylori* enhances cellular senescence in gastric mucosa via CXCR2 signaling.

Because *H pylori* infection is associated with both inflammation and DNA damage,<sup>26</sup> we also confirmed that mucosa with *H pylori* infection had more gamma H2A.X variant histone ( $\gamma$ H2ax)-positive cells (Figure 3K), as previously reported,<sup>27</sup> and DNA damage is a common stress of cellular senescence.<sup>28</sup> We investigated whether CXCR2 signaling was altered in GES-1 and AGS cells undergoing senescence induced by DNA damage. Our data show that CXCR2 and its ligands were up-regulated significantly (Figure 4A and B). Furthermore, overexpression of CXCR2 in both GES-1 and AGS cells enhanced DNA damage-induced senescence (Figure 4C and D), while knocking down CXCR2-attenuated senescence in the same model (Figure 4E and F). Importantly, CXCR2 knockdown or inhibition with SB225002 in vitro prevented the senescence enhanced by PMSS1 in AGS cells (Figure 4G). Collectively, these data indicate that *H pylori* enhances mucosal cell senescence via the CXCR2-associated signaling pathway.

### CXCR2 Expression Is Up-regulated Directly by NFKB1 Under *H pylori* Infection

Next, we investigated the possible mechanisms by which *H pylori* up-regulates CXCR2 expression. Because we found that CXCR2 was up-regulated at both the mRNA and protein levels, we hypothesized that CXCR2 most likely was up-regulated via transcription factors activated by *H pylori*. Therefore, we used PROMO and JASPAR to predict possible transcription factors that bind to the CXCR2 promoter region 2000 bp upstream and 500 bp downstream of the transcription start site. Transcription factors activated by *H pylori* were analyzed using GSE3556 from the GEO database with the GSEA gene set C3\_TFT. Based on these results, 7 transcription factors were included for further analyses (Figure 5A). We next explored the key transcription factors contributing to the function of *H pylori* using inhibitors or small interfering RNA and finally found that inhibition of the NF- $\kappa$ B signaling pathway most efficiently attenuated the up-regulated expression of CXCR2 induced by *H pylori* at the mRNA level (Figure 5B–D). An NF- $\kappa$ B signaling inhibitor was confirmed to have the same effect at the protein level (Figure 5E). Two transcription factors, RELA proto-oncogene, NF- $\kappa$ B subunit (RELA) and NFKB1, were predicted to be involved in the NF- $\kappa$ B pathway (Figure 5A, right panel). The NF- $\kappa$ B pathway is well known to be activated by *H pylori*.<sup>8</sup> To determine which transcription factor plays a critical role, AGS cells were transfected with either the RELA plasmid, NFKB1 plasmid, or a vector. In our study, NFKB1 was sufficient to up-regulate the expression of CXCR2, while RELA was not (Figure 5F and G). Luciferase experiments showed that of the 3 predicted NFKB1 binding sites we analyzed earlier (Figure 6A), the deletion of response elements 2 and 3 partly inhibited NFKB1 function. This indicates that response elements 2 and 3 might be the functional binding sites (Figure 6B and C). In addition, we confirmed that reporter activity increased in the same trend when AGS cells were infected with *H pylori* (Figure 6D), although no significant change was observed when 293T or AGS cells were transfected with the RELA plasmid

**Figure 2. (See previous page). *H pylori* promotes gastric epithelial cell senescence.** (A) Gram staining of PMSS1. (B) CXCL8 mRNA was measured using qPCR after AGS cells were infected with PMSS1 for 8 hours. Means  $\pm$  SD. Representative of 2 independent repeats analyzed by an unpaired *t* test. (C) NF- $\kappa$ B signaling was assessed using Western blot analysis after AGS cells were infected with PMSS1 for 8 hours. This process was repeated twice. (D) Schematic diagram of the *H pylori*-infected mouse model. (E) SA- $\beta$ -gal staining (left upper panel) and IHC staining of *H pylori* colonization (left lower panel) in the *H pylori*-infected and control mouse groups (samples are from antrum). Right: The histology score of *H pylori* colonization is shown. Plot: median. The red arrow refers to typical *H pylori* staining (S shape). Scale bar: 100  $\mu$ m (upper panel); 50  $\mu$ m (lower panel). (F) Senescent cells were detected by SA- $\beta$ -gal staining in mucosa samples from PMSS1-infected mice (*n* = 12). Quantification was performed according to pathologic types (the 4 diagnoses were defined according to the same strategy we used in Figure 1B; *n* = 12 for each category). Plot: median. Lower: Representative H&E images are shown. Black arrow: Typical goblet cells. Representative Alcian blue staining of goblet cells also is shown in the bottom right of the H&E image. Red arrow: Typical nuclear dysplasia. Scale bar: 100  $\mu$ m. All images were taken from the antrum except that images about IM were from the junction between the antrum and corpus. (G) Representative human mucosa samples (from antrum) negative and positive for *H pylori* infection as detected using IHC. (H) Senescent cells detected by Sudan Black B in *H pylori*-negative and *H pylori*-positive human precancerous lesions (from antrum). Senescent cells were analyzed only in atrophic mucosa without IM or DP. Samples from 20 patients diagnosed with CG, AG, IM, and DP. *n* (negative) = 11, *n* (positive) = 9. Plot: median. Mann-Whitney test. (I and J) SA- $\beta$ -gal staining and BrdU labeling in AGS and GES-1 cells. Cells were first exposed to 5 Gy radiation to induce senescence and then co-cultured with *H pylori* strain PMSS1 for 5 days (means  $\pm$  SD, unpaired *t* test). (G–J) Scale bar: 50  $\mu$ m. \**P* < .05. \*\**P* < .01. \*\*\*\**P* < .0001. GAPDH, glyceraldehyde-3-phosphate dehydrogenase; NFR, nuclear fast red; SBB, Sudan Black B.

(Figure 6E). Furthermore, chromatin immunoprecipitation (ChIP) analysis showed that NFKB1 could bind to response elements 2 and 3 (Figure 6F and G), which was consistent with the results of the luciferase assay. In the mouse model, Nfkb1 was significantly activated in mucosa with *H. pylori*

infection compared with mucosa under the control condition (Figure 6H). In addition, we observed the colocalization of high expression of *Cxcr2* and positive nuclear staining of Nfkb1 in the same area of the mucosa (the base of the mucosa glands, where there were obvious senescent cells)

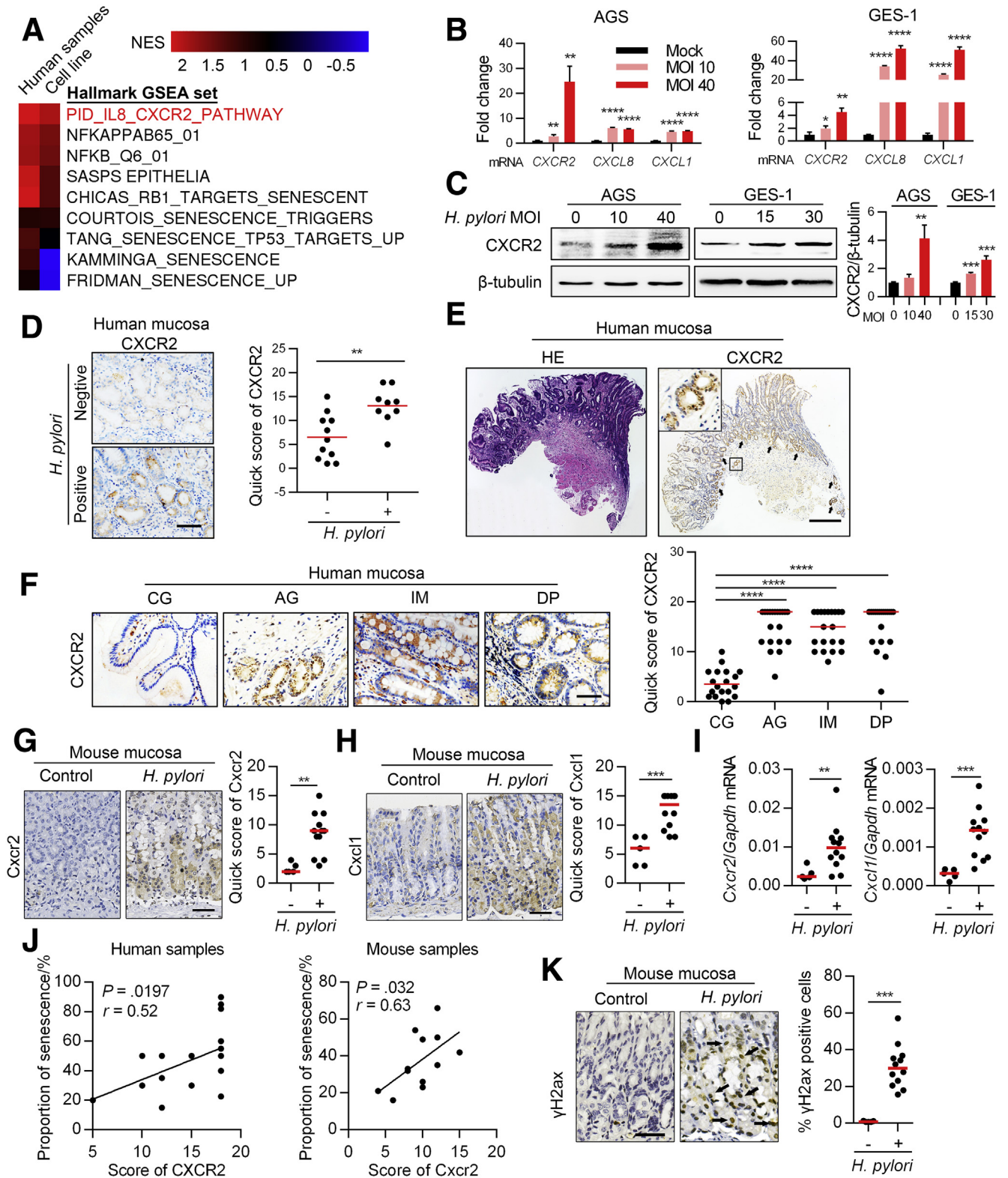


(Figure 2E) and a positive correlation between Cxcr2 protein level and Nfkb1 activation (Figure 6I). These results suggest that NFKB1 activated by *H pylori* binds directly to the CXCR2 promoter region and thus up-regulates CXCR2.

### CXCR2 Enhances the Senescence of Gastric Epithelial Cells via the p53–p21 Signaling Pathway

To identify the critical pathways on which CXCR2 depends to induce senescence in gastric epithelial cells, we measured the expression of important factors involved in senescence, including p53, p21, p27, p16, and retinoblastoma tumor-suppressor protein, using quantitative polymerase chain reaction (qPCR) in AGS cells undergoing senescence induced by DNA damage. We found that cyclin-dependent kinase inhibitor 1A (*CDKN1A*) mRNA (encoding p21) increased in both a dose-dependent and time-dependent manner, while tumor protein p53 (*TP53*) mRNA (encoding p53) increased only slightly (Figure 7A). RB transcriptional corepressor 1 mRNA (encoding retinoblastoma tumor-suppressor protein) also increased on day 6 after radiation, but there was no significant change in *CDKN1B* mRNA (encoding p27) and *CDKN2A* mRNA (encoding p16) (Figure 7A). P53, phos-p53 (p-p53, Ser15), and p21 protein expression interestingly were increased in both a dose-dependent and time-dependent manner (Figure 7B). These data indicated that p53–p21 signaling might be the key pathway mediating cellular senescence in gastric epithelial cells.

We next found that overexpression of CXCR2 slightly increased p53 expression, but there was a more apparent increase in phosphorylated p53 at serine 15. Phosphorylation of p53 at serine 392 also increased slightly (Figure 7C), while p21 expression increased significantly (Figure 7C). CXCR2 knockdown also resulted in consistent changes in p53 and phosphorylated p53 (Ser 15) expression (Figure 7D). Upon *H pylori* infection, p-p53 (Ser15) and p21 protein expression increased significantly (Figure 7E), which was consistent with a previous study.<sup>29</sup> Furthermore, knockdown of CXCR2 significantly suppressed p53–p21 signaling activation under *H pylori* infection (Figure 7F). In the mouse model, p21 protein levels

were up-regulated significantly in mucosa with *H pylori* infection compared with those under the control condition (Figure 7G). In addition, SA- $\beta$ -gal and bromodeoxyuridine (BrdU) staining showed that knockdown of p53 prevented CXCR2-enhanced senescence in AGS cells under radiation (Figure 8A), and knockdown of p53 inhibited the up-regulation of p21 by CXCR2 under this condition (Figure 8B).

To further confirm these findings, we evaluated the role of CXCR2 in the gastric cancer cell lines HGC27 and KATO III, which lack p53 protein expression (HGC27 has the insertion frameshift C.450 451insC, and KATO III has a deletion of exons 2–11 of *TP53*). Interestingly, p21 and cyclin D1 were not up-regulated in either cell line, while extracellular signal-regulated protein kinase 1/2 signaling pathways were activated in both cell lines, which was in contrast to AGS cells with wild-type p53 protein expression (Figure 8E). Furthermore, overexpression of CXCR2 promoted proliferation rather than senescence in HGC27 cells (Figure 8C and D). Finally, we analyzed the correlation of CXCR2 and p21 expression in patient samples. In addition to samples from the 20 patients mentioned earlier, we collected mucosa biopsy samples from another 20 patients diagnosed with *H pylori*-induced CG with IM and DP, but without pure AG, because we could not find additional patients diagnosed with pure AG. The increased number of patient samples enabled us to gain a more precise conclusion. IHC of serial sections showed a high positive correlation between p21 and CXCR2 (Figure 8F). Furthermore, high p21 expression was observed in the mucosa of patients with AG and IM, whereas p21 rarely was expressed in the mucosa of patients diagnosed with CG and DP (Figure 8G). This pattern of expression was similar to the pattern of senescent cells in the precancerous mucosa (Figure 1B). Together, these results suggest that CXCR2-enhanced senescence is dependent on p53–p21 signaling.

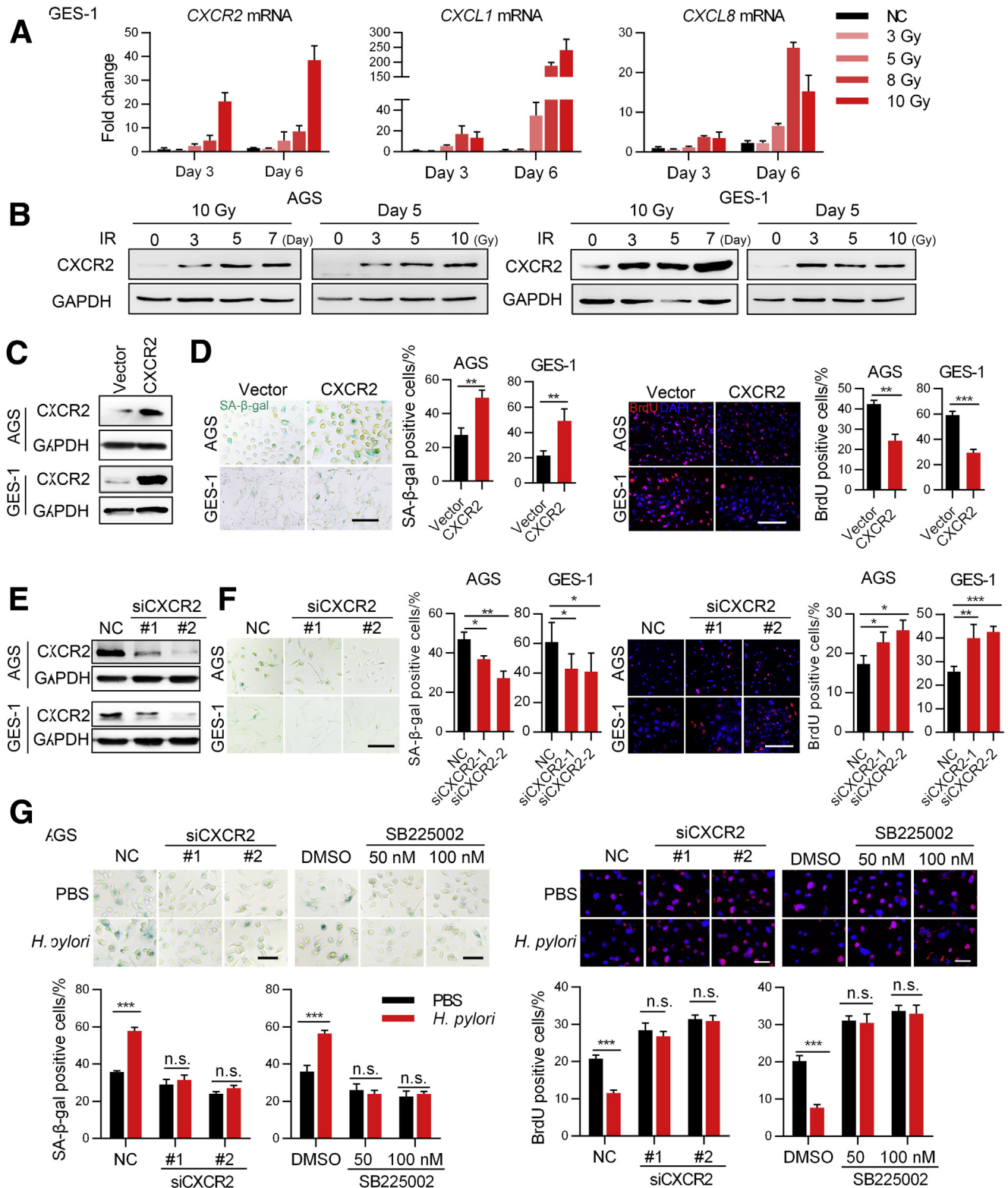
### Possible Positive Feedback Between p53 and CXCR2 Leads to Enhanced Senescence in Gastric Mucosa

Even after *H pylori* eradication, AG gastric lesions associated with this infection were not completely eliminated.<sup>30</sup>

**Figure 3. (See previous page). *H pylori* promotes gastric epithelial cell senescence via CXCR2 signaling.** Part A. (A) GSEA of senescence-associated pathways in *H pylori* infection using GSE47797 (human samples with *H pylori*-associated gastritis) and GSE3556 (AGS cell line infected with wild-type *H pylori* G27, which is CagA positive) from the GEO data set. NF- $\kappa$ B pathways were used as a positive control in the analyses. (B) Expression of CXCR2 and its important ligands was assessed using qPCR in gastric epithelial cell lines after infection with *H pylori* for 12 hours (means  $\pm$  SD, unpaired *t* test). (C) CXCR2 expression was assessed using Western blot analysis in gastric epithelial cell lines after infection with *H pylori*. qPCR and Western blot in (B and C) were repeated 3 times independently. (D) CXCR2 expression was evaluated using IHC in human gastric mucosa samples. Samples were grouped according to *H pylori* infection status, which was assessed via IHC as described in Figure 2G. Samples were from the 20 patients diagnosed with gastric precancerous lesions. *n* (*H pylori* negative) = 11, *n* (*H pylori* positive) = 9. Plot: median. IHC scores were analyzed using the Mann–Whitney test. (E) CXCR2 was highly expressed in atrophic glands, especially the base glands. *Black arrows*: typical atrophic glands. (F) CXCR2 expression was evaluated using IHC in different pathologic types of human tissue samples. Samples were from 20 patients diagnosed with CG, AG, IM, and DP. The 4 diagnoses were defined according to the same strategy we used in Figure 1B. *Left*: representative images. Plot: median. Mann–Whitney test. (G and H) IHC analysis of CXCR2 and CXCL1 in mouse mucosa (Mann–Whitney test). (I) qPCR analysis of *Cxcr2* and *Cxcl1* mRNA in mouse mucosa (Mann–Whitney test). (J) Correlation of CXCR2 and cellular senescence in human and mouse mucosa (Spearman test). (K) IHC of  $\gamma$ H2ax staining in mouse mucosa (Mann–Whitney test). *Black arrows*: typical nuclear staining of  $\gamma$ H2ax. All histology images were taken from the antrum. \**P* < .05. \*\**P* < .01. \*\*\**P* < .001. \*\*\*\**P* < .0001. NES, normalized enrichment score.

We therefore hypothesized that there is a positive feedback loop that remains active even after *H. pylori* infection is eliminated. A previous report showed that CXCR2 can be activated transcriptionally by p53.<sup>23</sup> Therefore, positive feedback between p53 and CXCR2 in gastric mucosa cells

could act as a critical enhancer of cellular senescence. To explore this hypothesis, we transfected 293T cells with lentivirus encoding wild-type p53, which resulted in increased CXCR2 mRNA levels (Figure 9B). We observed similar results for protein expression in 293T and AGS cells



transfected with lentivirus encoding p53 (Figure 9A). To evaluate whether the activation of endogenous p53 also could up-regulate CXCR2 expression, AGS cells were treated with the MDM2 proto-oncogene (MDM2) inhibitor Nutlin-3, which resulted in a time-dependent and dose-dependent increase in CXCR2 expression at both the mRNA and protein levels (Figure 9C and D). In contrast, knockdown of p53 in AGS cells attenuated the increased CXCR2 expression induced by DNA damage (Figure 9E). In the p53-deficient cell lines HGC27 and KATO III, DNA damage also caused senescence, but there was no increase in CXCR2 expression in the senescent cells (Figure 9F and G).

Using JASPAR and PROMO, we predicted 4 possible p53 binding sites in the CXCR2 promoter region (Figure 9H). We divided these 4 sites into 2 response elements based on distance (Figure 9H). ChIP analysis of these elements showed increased enrichment of response element 2 (Figure 9I). Our luciferase assay confirmed that deletion of the binding site located 54–68 bp upstream of the CXCR2 transcription start site completely reduced the luciferase activity enhanced by endogenous or exogenous p53 (Figure 9J and K). To evaluate whether the hypothesized positive feedback loop exists after *H pylori* eradication, CXCR2 and p53–p21 signaling were analyzed in AGS cells after antibiotic eradication and those with active *H pylori* infection. The results showed that both the CXCR2 level and p53–p21 signaling activation remained almost the same after *H pylori* eradication (Figure 9L). These results suggest that there might be a positive feedback loop between p53 and CXCR2 in gastric epithelial cells, which leads to enhanced senescence in gastric mucosa.

### Pharmaceutical Inhibition of CXCR2 Attenuates Cellular Senescence and Mucosa Atrophy Induced by *H pylori* In Vivo

Finally, we investigated whether inhibition of CXCR2 in the early stage of *H pylori* infection can efficiently attenuate excessive senescence in gastric mucosa cells, thus preventing mucosa senescence and AG using a mouse model infected with *H pylori* strain PMSS1 alone or with N-methyl-N-nitrosourea (MNU) (protocol is presented in Figure 10A). Patients with *H pylori* infection always experience other environmental risk factors. We used MNU as a DNA damage inducer to imitate other environmental risk factors to evaluate the effect of CXCR2 inhibition under conditions

more comparable with realistic conditions. It seemed that neither MNU nor the CXCR2 inhibitor SB225002 had a significant impact on *H pylori* colonization (Figure 10B). CXCR2 inhibitor treatment protected against neutrophil, but not monocyte, infiltration.<sup>31</sup> We observed notably decreased neutrophil scores in the groups treated with SB225002 (Figure 10C). In addition, our results showed that the percentage of senescent cells was decreased significantly in mice treated with SB225002, even in the PMSS1 combined with MNU group (Figure 10D). Next, we assessed the effect of the CXCR2 inhibitor on the development of different gastric precancerous lesions. The pathologic scores of tissue sections evaluated using H&E staining showed that scores for AG were lower in SB225002-treated mice than in untreated mice (Figure 11). Interestingly, we found that scores of IM and DP were also decreased significantly in SB225002-treated mice compared with control mice (Figure 11C). Collectively, these results suggest that treatment with the CXCR2 inhibitor in the early stage of *H pylori* infection efficiently attenuates neutrophil infiltration, cellular senescence, and mucosa atrophy, and might delay the progression of gastric precancerous lesions.

## Discussion

Previous studies have shown that the main cause of *H pylori*-induced AG is the activation of mechanisms associated with *H pylori* infection, including direct damage from *H pylori* attachment and subsequent inflammation and apoptosis.<sup>6,32</sup> In this study, we showed that cellular senescence is another newly defined important cause of *H pylori*-induced AG and that senescence in the gastric mucosa was associated strongly with *H pylori*-activated CXCR2 signaling. In our study, senescent cells were detected not only in the superficial glandular layer, but also throughout the whole gastric mucosa, especially the base of the glands, which are formed mainly by parietal cells and chief cells.<sup>8</sup> This suggests that even stem cells and progenitor cells in the bottom and isthmus of the glands undergo senescence. As has been shown previously, superficial and parietal cells are continuously lost,<sup>32</sup> and after a certain time the lack of new cells differentiating from progenitor or stem cells results in atrophy. This is the possible mechanism to explain why cellular senescence finally causes mucosa atrophy. Recently, it was reported that *H pylori* and AG were associated significantly with accelerated epigenetic aging.<sup>33</sup>

**Figure 4.** (See previous page). *H pylori* promotes gastric epithelial cell senescence via CXCR2 signaling. Part B. (A) qPCR and (B) Western blot showing changes in the expression of CXCR2 and its ligands in the DNA damage-induced senescence model (means  $\pm$  SD, unpaired *t* test). Two independent replicates were performed. (C) CXCR2 expression was evaluated using Western blot analysis after AGS and GES-1 cells were transfected with lentivirus encoding CXCR2. (D) SA- $\beta$ -gal and BrdU staining showing senescent cells. Cells were transfected with lentivirus encoding CXCR2 or a control vector and then exposed to 5 Gy X-ray, followed by culture for another 5 days before staining (means  $\pm$  SD, unpaired *t* test). Scale bar: 50  $\mu$ m. (E) Western blot analysis detecting CXCR2 expression in AGS and GES-1 cells transfected with CXCR2 small interfering (si)RNA or negative control sequences. (F) SA- $\beta$ -gal and BrdU staining showing senescent cells. Cells were exposed to 5 Gy X-ray after transfection and then cultured for another 5 days before staining (means  $\pm$  SD, unpaired *t* test). Scale bar: 50  $\mu$ m. (G) AGS cells were first transfected with CXCR2 siRNA or treated with SB225002 and then exposed to 5 Gy X-ray. After that, the cells were cocultured with PBS or PMSS1. SA- $\beta$ -gal staining and BrdU labeling were performed 5 days later (means  $\pm$  SD, unpaired *t* test). Scale bar: 20  $\mu$ m. All of the results are representative of 3 independent experiments. \**P* < .05. \*\**P* < .01. \*\*\**P* < .001. DMSO, dimethyl sulfoxide; GAPDH, glyceraldehyde-3-phosphate dehydrogenase; NC, negative control.

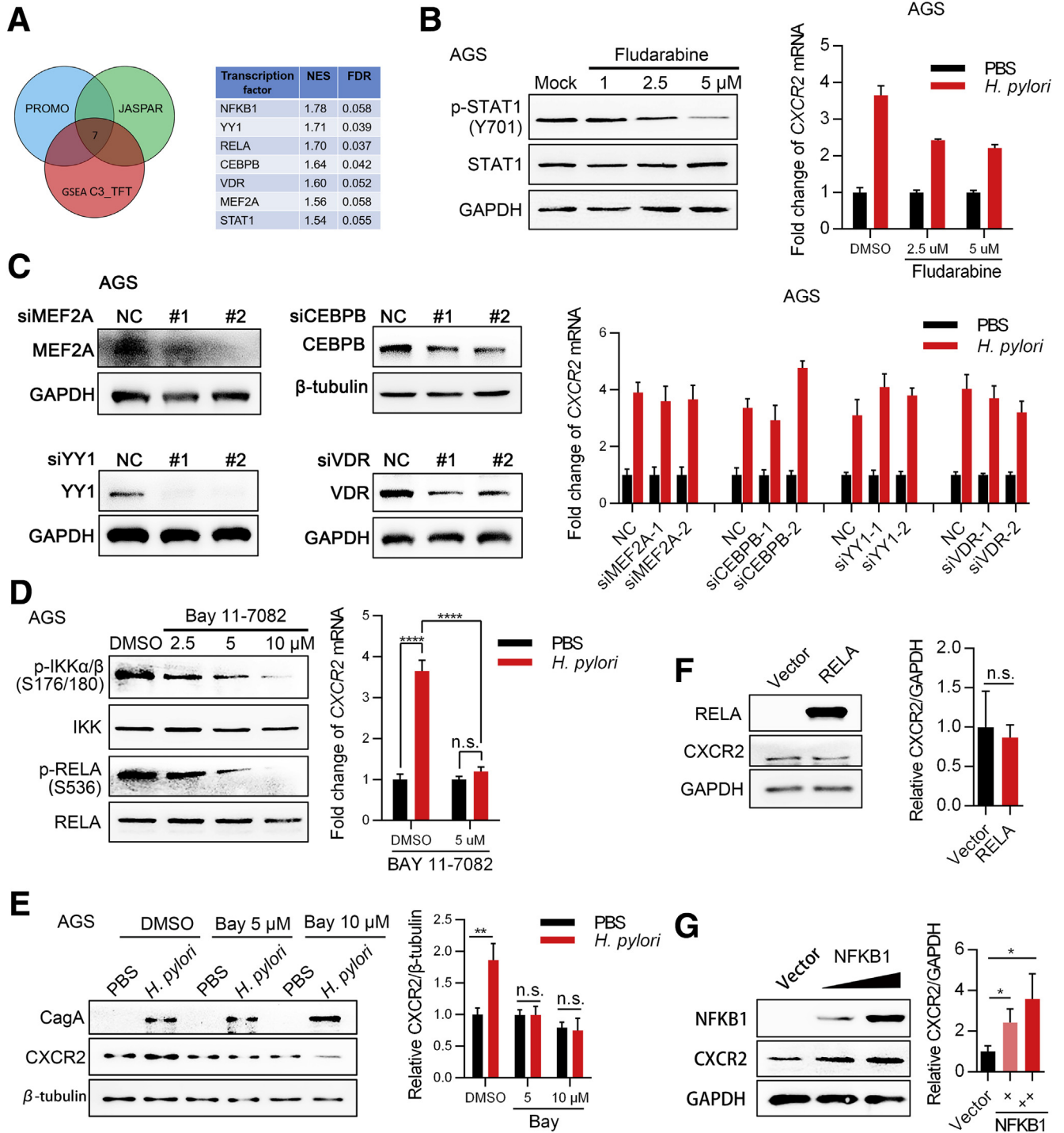
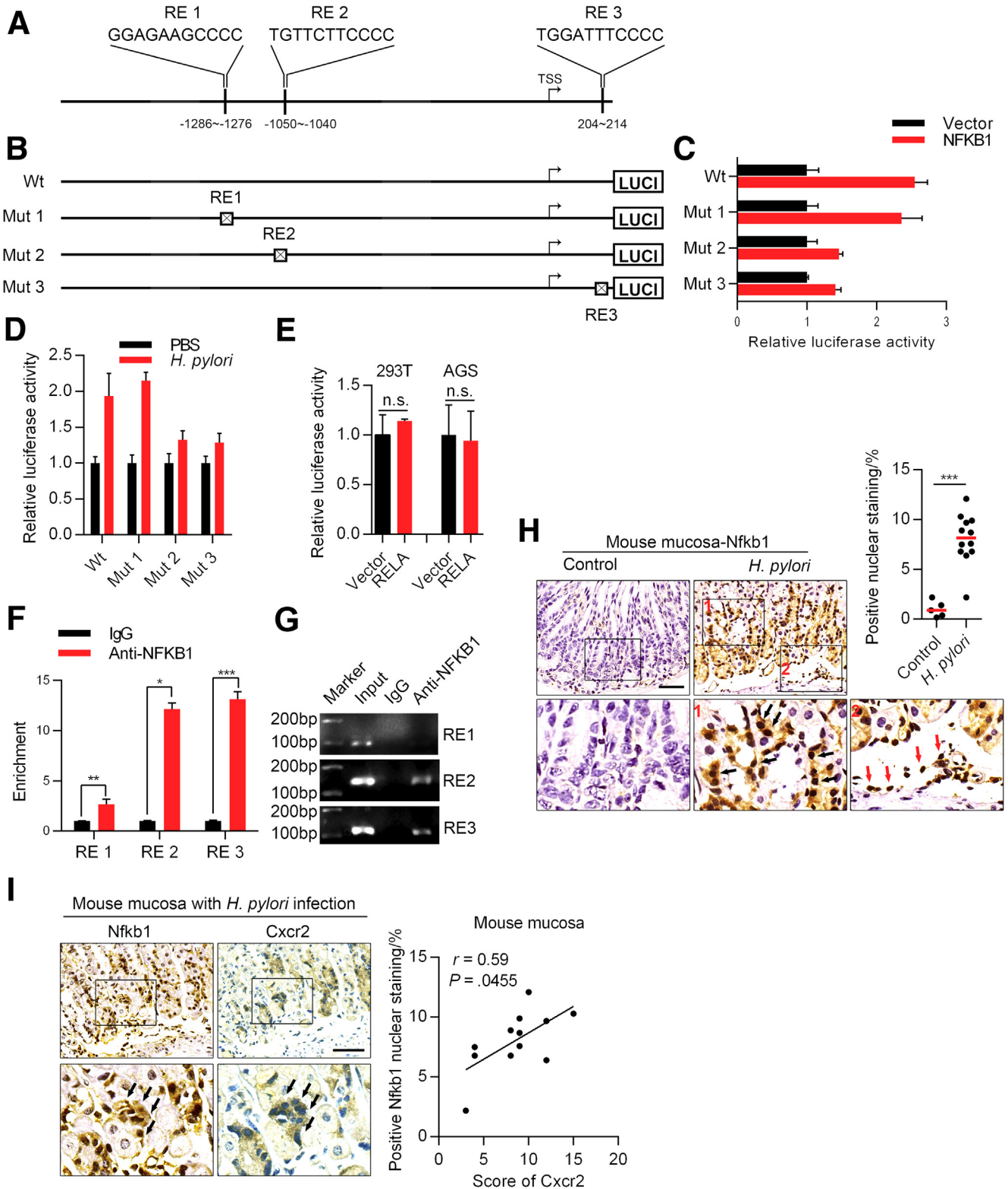


**Figure 5. *H. pylori* transcriptionally up-regulates CXCR2 expression via NFKB1.** (A) Transcription factors that were up-regulated by CagA and predicted to bind directly to the promoter region of CXCR2 according to the databases PROMO and JASPAR. For GSEA, the GEO data set GSE3556 was used. NES  $\geq$  1.5, NOM  $P$  value  $\leq$  .05, FDR  $\leq$  0.25. (B) Inhibition of the signal transducer and activator of transcription 1 (STAT1) pathway with fludarabine was evaluated in AGS cells using Western blot analysis (left panel). Cells were treated with fludarabine and then incubated with PMSS1 for 12 hours. Samples then were harvested for qPCR analysis of CXCR2 mRNA expression (right panel). Means  $\pm$  SD. (C) The efficiency of several small interfering (si)RNAs was evaluated using Western blot analysis in AGS cells (left). AGS cells were transfected with siRNA for 48 hours and then incubated with PMSS1 for 12 hours. Samples then were harvested for qPCR analysis of CXCR2 mRNA (right panel). Means  $\pm$  SD. (D and E) Inhibition of the NF- $\kappa$ B signaling pathway with Bay11-7082 for 14 hours in AGS cells was evaluated using Western blot analysis. For *H. pylori* infection, AGS cells were first treated with BAY 11-7082 for 2 hours, followed by *H. pylori* infection for 12 hours. (D) Right: means  $\pm$  SD, unpaired  $t$  test. (E) Cells under the same conditions also were harvested for Western blot analysis. (F) AGS cells were transfected with RELA or vector plasmid for 48 hours and then collected for Western blot analysis. (G) AGS cells were transfected with the NFKB1 plasmid for 48 hours and then collected for Western blot analysis. All the Western blot and qPCR results were repeated 3 times. \* $P$  < .05. \*\* $P$  < .01. \*\*\*\* $P$  < .0001. CEBPB, CCAAT enhancer binding protein beta; DMSO, dimethyl sulfoxide; GAPDH, glyceraldehyde-3-phosphate dehydrogenase; NC, negative control; VDR, vitamin D receptor.

which indicated a complex role of *H. pylori* in senescence and aging.

Our data also suggest that *H. pylori* activates positive feedback between p53 and CXCR2, which continues to

enhance cellular senescence. We also showed that this positive feedback was activated by NFKB1, which transcriptionally increased the expression of CXCR2. NFKB1 can be activated by various inflammatory factors, such as tumor necrosis



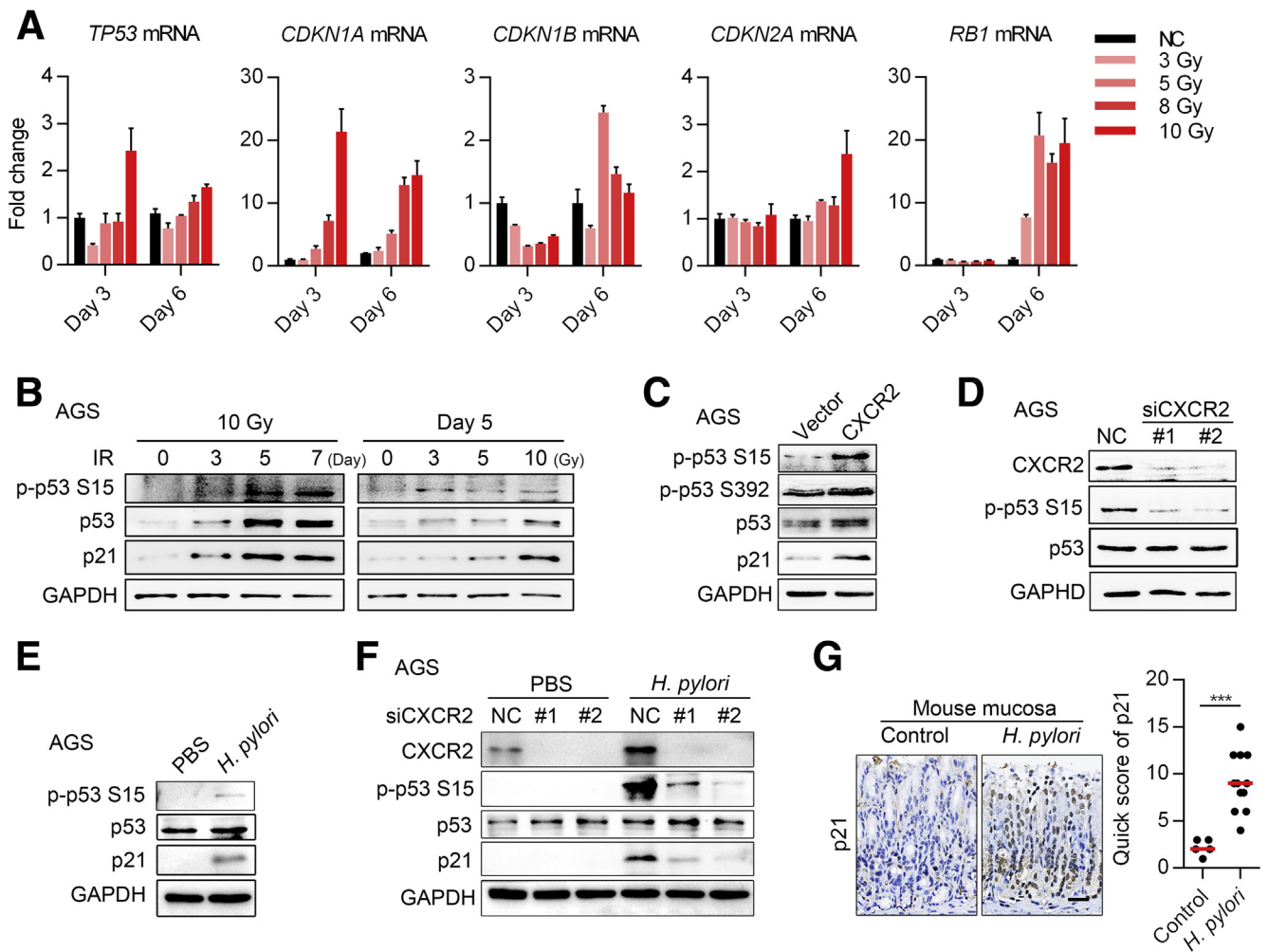


**Figure 7. *H. pylori* infection activates p53–p21 signaling.** (A) Expression of major senescence-associated genes as assessed using qPCR in X-ray-induced senescence in GES-1 cells (means  $\pm$  SD). (B) Expression of the p53 pathway detected using Western blot analysis in AGS cells. Both qPCR and Western blot results are representative of 2 independent experiments. (C) Western blot analysis of proteins involved in the p53-associated senescence pathway in AGS cells overexpressing CXCR2. (D) Western blot analysis of proteins involved in the p53-associated senescence pathway after CXCR2 knockdown using small interfering (si)RNA. (E) Activation of p53–p21 signaling was analyzed by Western blot upon *H. pylori* (MOI, 100) infection for 3 hours. (F) AGS cells were first transfected with CXCR2 siRNA for 48 hours, followed by *H. pylori* (MOI, 100) infection for 3 hours. Samples then were harvested for Western blot analysis. (G) IHC analysis of p21 in mouse mucosa (from antrum). Scale bar: 100  $\mu$ m. \*\*\* $P$  < .005. GAPDH, glyceraldehyde-3-phosphate dehydrogenase; NC, negative control.

**Figure 6. (See previous page). NFKB1 directly up-regulates CXCR2.** (A) Diagram showing the NFKB1 transcription response element (RE) in the CXCR2 promoter region predicted by PROMO and JASPAR. (B) Diagram of wild-type (Wt) and mutant (Mut) reporters. Each predicted RE was deleted in 1 mutant reporter. (C) Relative luciferase activity of different promoters in 293T cells transfected with the NFKB1 plasmid or empty vector (means  $\pm$  SD). (D) Relative luciferase activity of the wild-type and mutant promoters in AGS cells infected with *H. pylori* or PBS for 48 hours. (E) Relative luciferase activity of the wild-type promoter in 293T and AGS cells transfected with RELA plasmid or empty vector. Luciferase experiments were performed 3 times and analyzed with an unpaired  $t$  test. (F) Enrichment of the 3 predicted response elements from ChIP analysis (repeated twice, means  $\pm$  SD, unpaired  $t$  test). (G) DNA agarose gel electrophoresis displaying representative results from 2 independent ChIP experiments. (H) IHC analysis of NFKB1 in mouse mucosa (from antrum, Mann–Whitney test). Black arrows show typical positive nuclear staining of NFKB1. Red arrows show positive control of NFKB1 nuclear staining in the infiltrated immunocytes. (I) Positive correlation between Nfkb1 activation and Cxcr2 levels (Spearman test). Left: Representative images of Nfkb1 and Cxcr2 staining from serial sections are shown (from antrum). Black arrows show representative glands where there is positive Nfkb1 nuclear staining and high expression of Cxcr2 protein. Scale bar: 50  $\mu$ m. \* $P$  < .05. \*\* $P$  < .01. \*\*\* $P$  < .001. LUCI, luciferase.

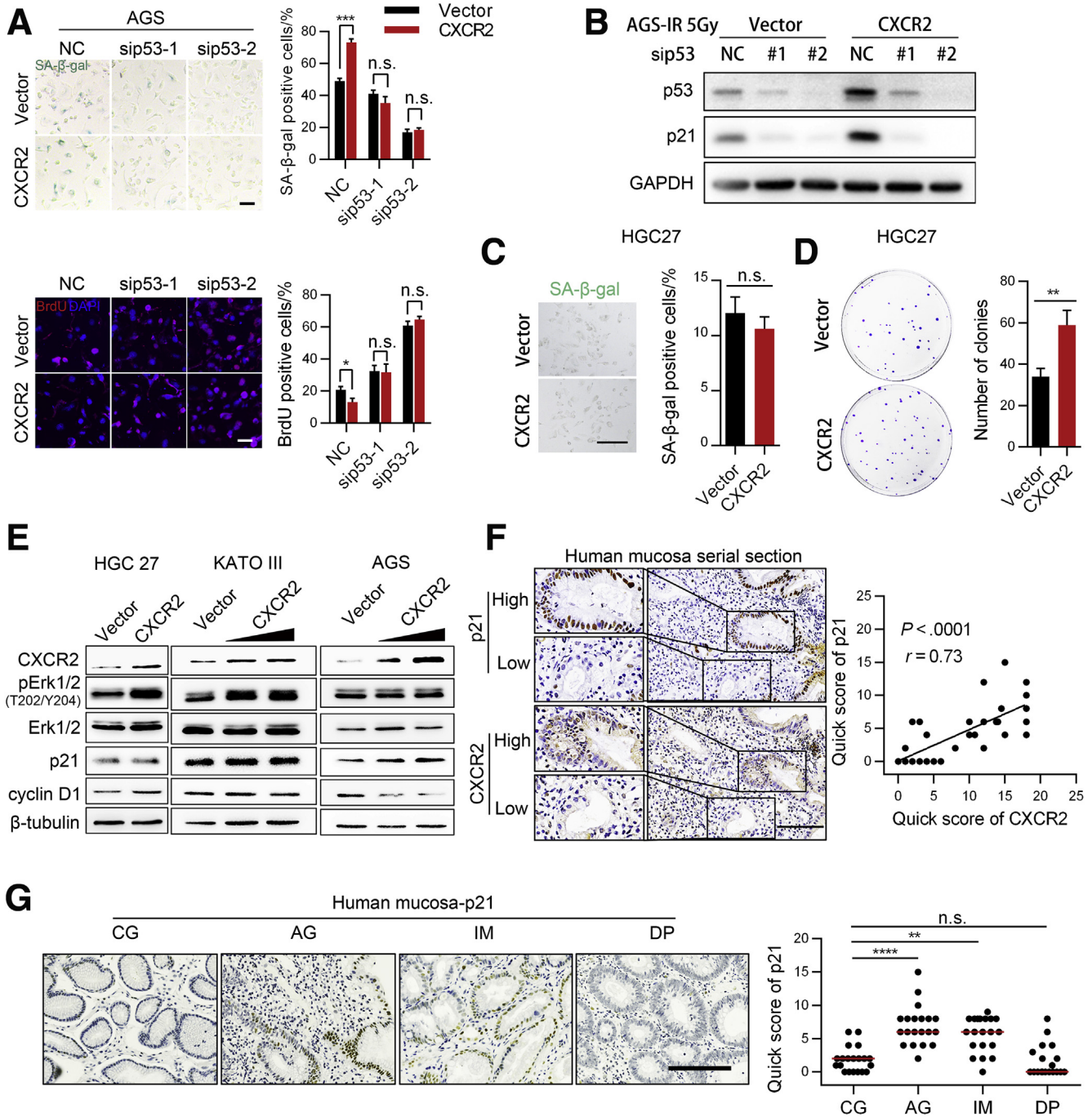
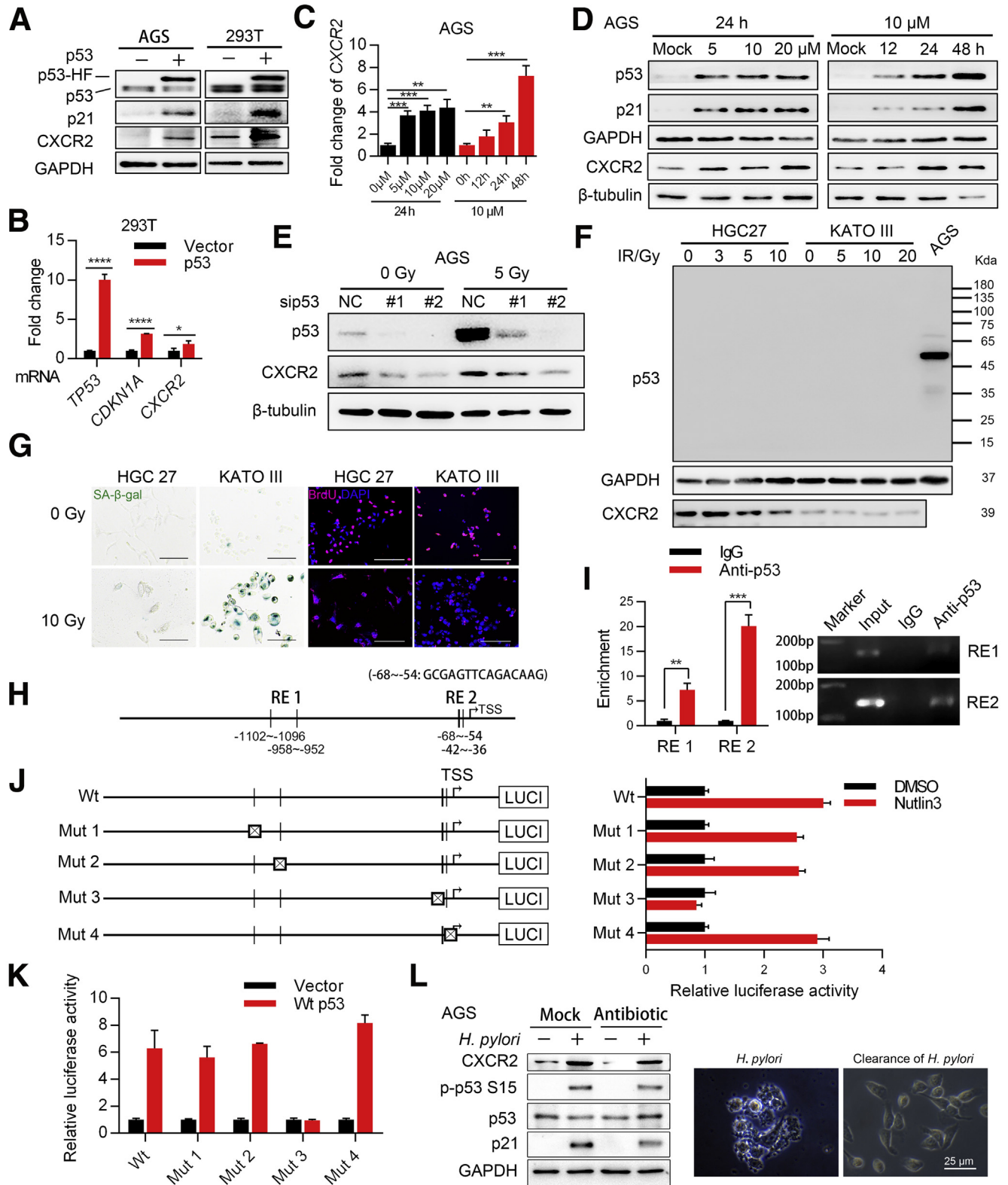


**Figure 8. CXCR2 promotes gastric epithelial senescence through p53-p21 signaling.** (A and B) SA-β-gal and BrdU staining of AGS cells cotransfected with lentiviruses encoding CXCR2 and small interfering (si)RNA targeting *TP53* mRNA for 24 hours, followed by radiation (5 Gy, means ± SD, unpaired *t* test). Staining was performed 5 days later. Scale bar: 50 μm. Data are representative of 3 independent experiments. Unpaired *t* test. (B) Representative Western blot images of p53 and p21 under this condition are shown. (C) SA-β-gal staining analysis of HGC27 cells transfected with lentiviruses encoding CXCR2. Cells were stained 5 days after exposure to 5 Gy X-ray. Scale bar: 50 μm. Means ± SD. Unpaired *t* test. (D) Plate colony formation assay of HGC27 cells transfected with lentiviruses encoding CXCR2. Only clones with a parameter greater than 1 mm were counted. (C) SA-β-gal staining and (D) colony formation were repeated twice independently. (E) Western blot analysis of several key proteins in proliferation-associated pathways in HGC27, KATO III, and AGS cells transfected with lentiviruses encoding CXCR2. All Western blot results shown are representative samples from 3 independent experiments. (F) Quick scores of CXCR2 and p21 in precancerous lesions from the 40 patients as determined by IHC staining. CXCR2 and p21 staining were performed in adjacent slices. Correlations were analyzed by the Spearman test. Left: Representative images are shown. (G) p21 expression in human precancerous lesions as detected by IHC (samples from 20 patients diagnosed with CG, AG, IM, and DP). Scale bar: 100 μm. Plot: median. Mann-Whitney test. All histology images were taken from the antrum. \*\**P* < .01. \*\*\**P* < .001. \*\*\*\**P* < .0001. GAPDH, glyceraldehyde-3-phosphate dehydrogenase; NC, negative control.

factor- $\alpha$  induced by *H pylori* infection<sup>7</sup> or IL1- $\alpha$  from SASP, which suggests that once abundant senescence is activated, *H pylori* is no longer necessary for the maintenance of mucosa senescence. Thus, these results might explain why *H pylori*

eradication has little or no effect in clinical practice after patients are diagnosed with apparent atrophy.<sup>30,34-36</sup>

The present study also shows that *H pylori*-induced senescence in the mucosa is dependent on wild-type



p53–p21 signaling. Meanwhile, an increased frequency of *TP53* gene mutations was reported previously in gastric tissue from AG to gastric cancer patients.<sup>37</sup> *TP53* mutations in gastric mucosa were associated strongly with *H pylori* infection,<sup>38,39</sup> which caused DNA damage<sup>40</sup> and up-regulated the expression of activation-induced deamination.<sup>41</sup> Activation-induced deamination converts cytosine into uracil, which is replaced by a thymine after DNA replication.<sup>42</sup> Therefore, *H pylori* infection induces the most common *TP53* mutation type: the missense mutation. These results indicate that *H pylori* has 2 conflicting roles in gastric tumorigenesis: *H pylori* enhances senescence while also inducing *TP53* mutations to disrupt senescence. This suggests that a *TP53* mutation might be the main mechanism underlying gastric epithelial cell escape from senescence, acting as a kind of switch that activates progression from AG to IM or DP. In addition, the sequential increase in *TP53* mutation from AG to gastric cancer may explain why high CXCR2 expression was detected in IM and DP, but the number of senescent cells decreased.

If AG is caused by excessive senescence, then inhibiting CXCR2 might prevent AG. Consequently, prevention of AG might delay the progression of advanced precancerous lesions. Our results from the *H pylori*-infected mouse model supported this hypothesis. This hypothesis is based on the evidence that IM develops from AG, which is induced or accelerated by some abnormal stimuli, such as CagA, acid, base, and alcohol.<sup>43</sup> During AG, loss of surface and parietal cells might expose gastric isthmus stem cells or chief cells to these stimuli and increase the risk of metaplasia.<sup>44,45</sup> Inhibiting senescence in gastric mucosa could reduce SASP, which could be correlated with inflammation, as is the case with gastric carcinogenesis.<sup>46</sup> Moreover, we showed that CXCR2 was critical for *H pylori*-mediated senescence and could form a positive feedback loop with p53. CXCR2 inhibition effectively prevented *H pylori*-mediated senescence and disrupted the positive feedback loop; however, CXCR2 inhibition did not stop p53 from inducing senescence because CXCR2 acts as an enhancer of p53. Therefore, based on these findings, we propose a model in which inhibition of CXCR2 prevents excessive senescence and

atrophic mucosa. For the in vivo studies, we did not produce a transgenic animal model in which CXCR2 was specifically knocked out in gastric mucosa cells because CXCR2 knockout is unfeasible in a clinical trial. We chose to use a CXCR2 inhibitor because this was more consistent with clinical application. We hope to provide evidence for further clinical trials.

One of the limitations of our study was that the impact of *H pylori* cytotoxic factors on cellular senescence was not evaluated. Epidemiologic studies have shown that the cytotoxic factors CagA and vacuolating cytotoxin A are associated with a higher frequency of AG.<sup>47</sup> In addition, CagA is an important activator of NF- $\kappa$ B signaling<sup>48</sup> and induces cellular senescence via the regulation of p21,<sup>18</sup> and it seems that CagA is able to activate CXCR2 signaling and thus promote cellular senescence. Overall, there is still much work to do to determine the role of *H pylori* cytotoxic factors in mucosa senescence and atrophy. The answer to this question may be useful for understanding the variation in AG in *H pylori*-infected patients. Another limitation was that the mechanisms by which CXCR2 regulates the protein level and Ser15 phosphorylation of p53 are still not clear and deserve further research in the future.

## Conclusions

In conclusion, this study shows that cellular senescence is a newly identified cause of *H pylori*-induced AG and that *H pylori* promotes gastric mucosa senescence via CXCR2 signaling. Pharmaceutical inhibition of CXCR2 attenuates mucosa senescence and atrophy induced by *H pylori* in vivo and might further delay the progression of precancerous lesions. CXCR2 therefore may be considered a potential target for tumor prevention strategies to decrease the risk of gastric precancerous lesions progressing to cancer.

## Methods

### Patients

We collected human gastric biopsy samples from 41 patients from the Endoscopy Center of the First Affiliated Hospital of Sun Yat-sen University. The study was approved by the Institutional Ethical Committee of the First Affiliated Hospital of Sun Yat-sen University (reference number: [2017]

**Figure 9. (See previous page). CXCR2 forms a positive feedback loop with p53 to enhance the cellular senescence of gastric epithelial cells.** (A) Western blot analysis of CXCR2 expression in AGS and 293T cells transfected with lentiviruses encoding p53. (B) qPCR analysis of CXCR2 mRNA expression in 293T cells transfected with p53 (*CDKN1A* mRNA, encoding p21, was used as a positive control, means  $\pm$  SD, unpaired *t* test). (C and D) qPCR and Western blot analyses of CXCR2 expression in AGS cells treated with Nutlin-3 in a time-dependent and dose-dependent manner. (E) Western blot analysis of p53 and CXCR2 expression in AGS cells transfected with p53 small interfering (si)RNA followed by radiation treatment. (F) Western blot analysis of CXCR2 in the HGC27 and KATO III cell lines after X-ray exposure. (G) SA- $\beta$ -gal and BrdU staining of senescent HGC27 and KATO III cells after X-ray exposure. Scale bar: 50  $\mu$ m. Repeated once. (H) Diagram showing the p53 transcription response element (RE) predicted by JASPAR and PROMO. (I) Enrichment scores of different REs obtained from ChIP analysis (means  $\pm$  SD, unpaired *t* test) and exemplary DNA agarose gel electrophoresis images from 2 independent repeats. (J) Left: diagram of wild-type (Wt) and 4 mutant (Mut) reporters. Each predicted RE was deleted in 1 mutant reporter. Right: Relative luciferase activity of different promoters in AGS cells treated with Nutlin-3 (10  $\mu$ mol/L) for 48 hours (means  $\pm$  SD). (K) Relative luciferase activity of different promoters in 293T cells transfected with vector or wild-type p53 plasmid. Means  $\pm$  SD. Luciferase data are representative of 3 independent repeats. (L) AGS cells were first infected with PMSS1 (MOI, 100) for 3 hours and then eradicated by antibiotics (penicillin and streptomycin) for 3 hours. Samples then were harvested, analyzed by Western blot, and compared with samples with active *H pylori* infection for 6 hours. Right: Representative images of AGS cells with *H pylori* infection and after *H pylori* eradication are shown. \**P* < .05. \*\**P* < .01. \*\*\**P* < .001. \*\*\*\**P* < .0001. DMSO, dimethyl sulfoxide; GAPDH, glyceraldehyde-3-phosphate dehydrogenase; HF, His-Flag; LUCI, luciferase; NC, negative control.

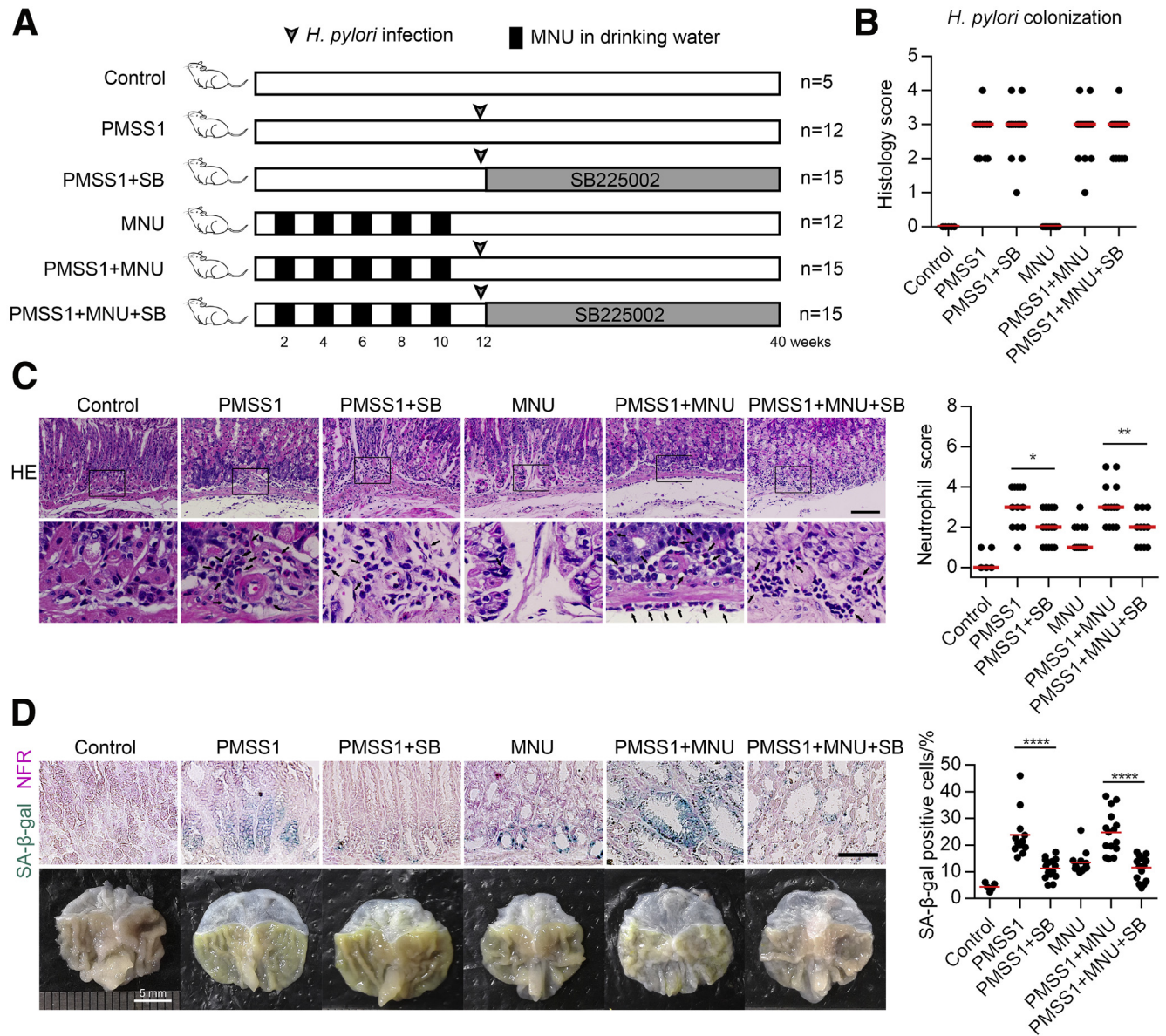


**Figure 10. Pharmaceutical inhibition of CXCR2 attenuates gastric mucosa senescence and atrophy in vivo.** (A) Diagram showing the protocol of the mouse study. (B) Colonization of *H. pylori* in different groups assessed by histology score. (C) Neutrophil infiltration score in different groups. *Left*: Representative H&E images are shown. *Black arrows*: neutrophils. *Scale bar*: 100  $\mu\text{m}$ . (D) *Upper*: Senescent cells detected using SA- $\beta$ -gal staining in mouse gastric mucosa in different groups. *Lower*: Representative images of mouse stomachs. *Scale bar*: 50  $\mu\text{m}$ . Plot: median. Significant differences were analyzed using the Mann-Whitney test. All histology images were taken from the antrum or the junction between the antrum and corpus. \* $P < .05$ . \*\* $P < .01$ . \*\*\*\* $P < .0001$ . NFR, nuclear fast red; SB, SB225002.

095), and informed consent was obtained from all patients. Of the 41 patients included in this study, 20 were diagnosed with CG combined with AG, IM, and DP. Twenty patients were diagnosed with CG combined with IM and DP. These samples were formalin-fixed and paraffin-embedded from October 2014 to April 2016. The inclusion criteria were as follows: patients with samples containing at least 2 types of gastric precancerous lesions (AG, IM, and DP); at least 3 biopsy samples from the gastric antrum or the gastric angle. The exclusion criteria were as follows: patients with autoimmune diseases, pernicious anemia, gastric surgery history, or

nonsteroidal anti-inflammatory drug use for more than 1 year, and patients with bile reflux disease. Because SA- $\beta$ -gal staining could not be performed on paraffin-embedded samples, only Sudan Black B staining was used to detect senescent cells in these samples. We only obtained fresh gastric biopsy samples from 1 patient in October 2017 who was diagnosed with CG combined with AG and IM. We performed SA- $\beta$ -gal staining on samples of this patient to detect senescent cells. When analyses were performed, histologic type was confirmed by H&E staining in the adjacent slice by 2 pathologists. CG was restricted to mucosa without AG, IM, or

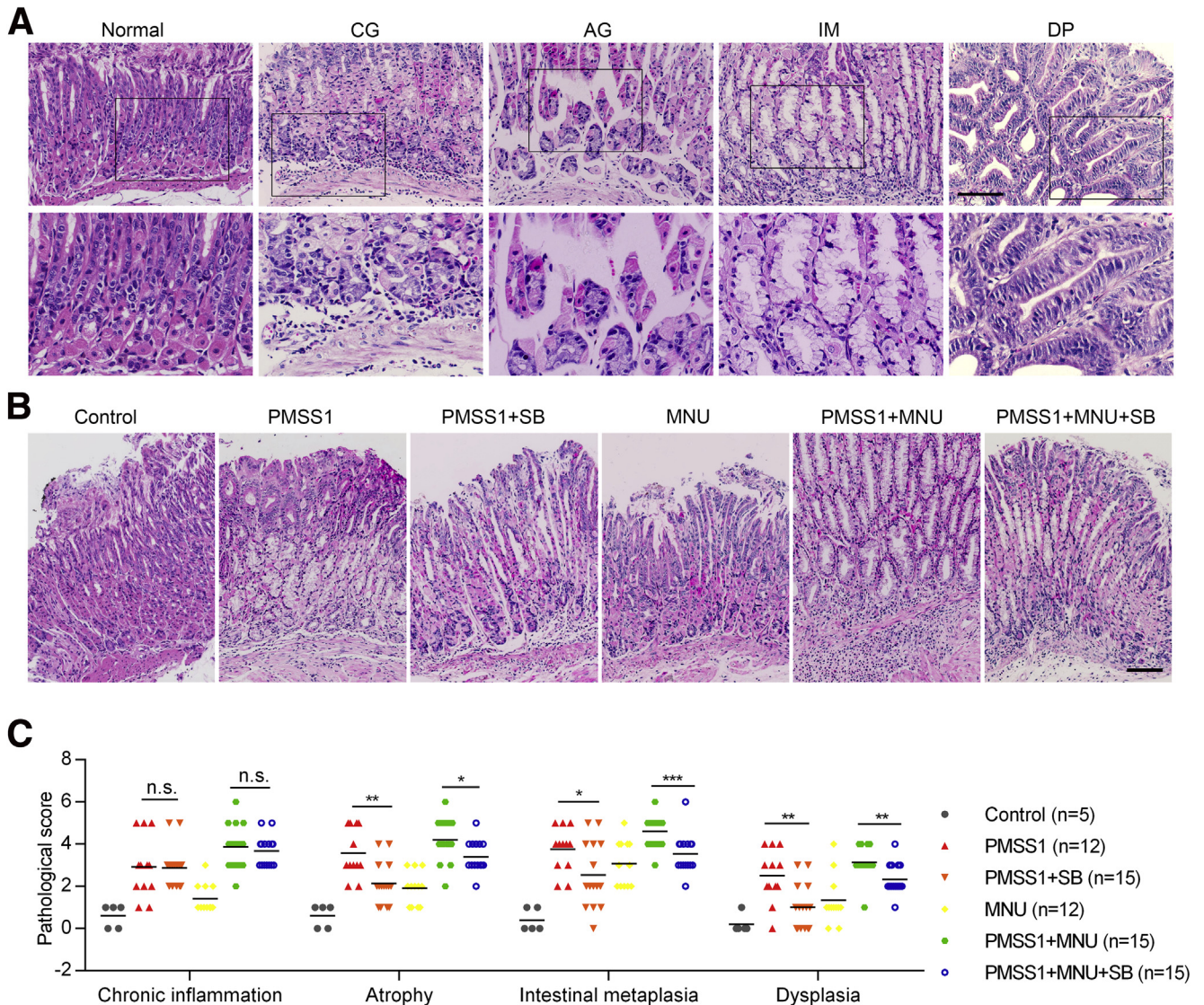


**Figure 11. Inhibition of CXCR2 delays the progression of gastric precancerous lesions in an *H. pylori*-infected mouse model.** (A) Representative H&E image of different lesions observed in the stomach of the mice. All images were taken from the antrum except that representative images showing IM were taken from the corpus. (B) Representative H&E staining images of different groups. The representative images of PMSS1+MNU and PMSS1+MNU+SB groups were taken from the corpus or the junction between the corpus and antrum, and other images were taken from the antrum. (C) Histologic score in different groups based on pathologic types. Scale bar: 100  $\mu\text{m}$ . Plot: median. Significant differences were analyzed using the Mann–Whitney test. \* $P < .05$ . \*\* $P < .01$ . \*\*\* $P < .005$ . SB, SB225002.

DP. AG was restricted to atrophic mucosa without IM or DP. IM was restricted to mucosa without DP.

### Cell Lines

The gastric cancer cell lines AGS, HGC27, and KATO III, and the embryonic kidney cell line 293T were purchased from the Cell Bank of the Typical Culture Preservation Committee, Chinese Academy of Sciences (Shanghai, China). The normal gastric epithelial cell line GES-1 was purchased from the Lab Animal Center of the Fourth Military Medical University (Shanxi, China). GES-1 and AGS cells were cultured in RPMI-1640 medium, HGC27 cells were cultured in Dulbecco's modified Eagle medium,

and KATO III cells were cultured in IMDM medium (Gibco-BRL, Grand Island, NY). Each culture medium was supplemented with 10% fetal bovine serum (Biological Industries, CT) and 1% antibiotics (100 U/mL penicillin and 100  $\mu\text{g}/\text{mL}$  streptomycin).

### SA- $\beta$ -gal and Sudan Black B Staining

To detect senescent cells, we used the SA- $\beta$ -gal Staining Kit (C0602 Beyotime; Shanghai, China) according to the manufacturer's instructions. Sudan Black B staining (GENMED, Shanghai, China) was conducted as described previously.<sup>49</sup> A total of 1000 cells were counted for each sample using light microscopy.

**Table 1.** siRNA Information

Target gene	Sequence
CXCR2-#1	GCTACTTGGTCAAATTCAT
CXCR2-#2	GCTATACATGGCTTGATCAGC
MEF2A-#1	GCTCAACGTTAACAGATTC
MEF2A-#2	GAAACCAGATCTTCGAGTT
CEBPB-#1	GCCCTGAGTAATCGCTTAA
CEBPB-#2	GTGGCCAACTTCTACTACG
YY1-#1	CGACGACTACATTGAACAA
YY1-#2	CCTGAAATCTCACATCTTA
VDR-#1	GTCAGTTACAGCATCCAAA
VDR-#2	CCCACCATAAGACCTACGA
TP53-#1	GAGAAUUAUUACCCUUAA
TP53-#2	UGGUUCACUGAAGACCCAGUU

siRNA, small interfering RNA.

### Lentiviral Transduction, Plasmid Transfection, and RNA Interference

The CXCR2 and RELA genes were cloned into the pEZ-Lv201 lentivirus vector (GeneCopoeia, Guangzhou, China), and NFKB1 and wild-type p53 were cloned into the pEnter lentivirus vector (Vigene Biosciences, Shandong, China). Small interfering RNAs for CXCR2, p53, MEF2A, CEBPB, YY1, and VDR were purchased from RiboBio (Guangzhou, China). Lentiviruses were transfected with MOI from 10 to 100, depending on the cell line, and 48 hours after transfection, cells were selected by puromycin to form stable cell lines. Plasmids and small interfering RNA were transfected with Lipofectamine 3000 reagent (Invitrogen), and 24 hours after transfection, the cell culture medium was replaced with fresh media. Sequences of small interfering RNA used were listed in Table 1.

### BrdU Incorporation

Cells were seeded on chamber slides (NEST, Wuxi, China), cocultured with BrdU for 5 hours (60  $\mu$ g/mL), washed with phosphate-buffered saline (PBS), and fixed with methanol for 5 minutes at room temperature in the dark. Slides were washed with PBS and incubated with PBS containing 2 mol/L HCl and 0.1% Tween 20 to break the double-stranded DNA. Next, 0.1 mol/L sodium borate was used to stop the reaction, and slides were washed in PBS, followed by incubation in 0.1% Tween 20 mixed with 10% goat serum to increase the permeability of the nuclear membrane and to block nonspecific antibody binding. The slides were incubated with anti-BrdU antibody overnight at 4°C and then with Alexa Fluor 594 goat anti-rat IgG (1:500) secondary antibody at room temperature for 1 hour. The slides then were incubated with 4',6-diamidino-2-phenylindole at room temperature for 15 minutes to visualize DNA. Finally, the slides were fixed with mounting medium (p36934; Invitrogen).

### Plate Colony Formation Assay

Cells transfected with CXCR2-encoding or control lentivirus were seeded in 6-well plates (500 cells/well) and then cultured for 2 weeks. After that, the cells were fixed with 10% (w/v) formaldehyde and stained with 1% (w/v) crystal violet for 60 minutes at room temperature.

### Quantitative Real-Time PCR

TRIzol reagent (Invitrogen) was used to extract RNA from gastric cancer cell lines and tissue samples according to the manufacturer's instructions. A Nanodrop 2000 (ThermoFisher, MA) and agarose gel electrophoresis were used to evaluate RNA quantity and quality. RNA was reverse-transcribed using Prime-Script RT Master Mix (RR036A; Takara, Shiga, Japan), and qPCR was performed using SYBR Premix Ex Taq (Tli RNaseH Plus, RR820A; Shiga, Japan) in an ABI 7900 (Applied Biosystems, MA) following the manufacturer's protocols. The relative mRNA expression levels of the target genes were calculated using the  $2^{-\Delta\Delta CT}$  method, and glyceraldehyde-3-phosphate dehydrogenase was used as an endogenous control. The primers used for the qPCR analysis are listed in Table 2.

### IHC Analysis

Four-micrometer-thick sections were deparaffinized in xylene and rehydrated in alcohol. Antigen retrieval was performed in citric acid (pH 6.0) or EDTA buffer (pH 8.9) in which sections were autoclaved for 2 minutes and placed in 3% H<sub>2</sub>O<sub>2</sub> at room temperature for 15 minutes to quench endogenous peroxidases. To block nonspecific antibody binding and increase the permeability of the nuclear membrane, sections were incubated in 10% goat serum-0.1% Tween 20 for 30 minutes. Finally, the slides were incubated with appropriate primary antibodies (Table 3) for 24 hours at 4°C in a humidified chamber. The next day, the slides were washed in PBS 3 times and incubated with horseradish-peroxidase-conjugated secondary antibody for 30 minutes followed by diaminobenzidine tetrahydrochloride chromogen (GK500710; GeneTechnology, Shanghai, China) at room temperature. Finally, the slides were counterstained with Mayer's hematoxylin, dehydrated, and mounted in neutral balsam before being scanned under the microscope (Axio Scan Z1, Zeiss, Oberkochen, Germany). Two pathologists reviewed and evaluated the cell staining independently, according to a previously reported protocol (quick score)<sup>50</sup>: the proportion of cells positively stained throughout the section was termed category A and was assigned scores from 1 to 6 (1, 0%–4%; 2, 5%–19%; 3, 20%–39%; 4, 40%–59%; 5, 60%–79%; and 6, 80%–100%). The average intensity, corresponding to the presence of negative, weak, intermediate, and strong staining, was given a score from 0 to 3 and termed category B. The quick score was a product of A  $\times$  B.

### Histologic Score Analysis of Gastric Mucosa Samples From Animal Models

Histologic scores were analyzed according to a protocol modified from a previous study.<sup>51</sup>

**Table 2.** Antibody Information

Antibody	Final dilution	Manufacturer and cat no
p53	Western blot (WB) 1:4000, IHC 1:1500	Abcam ab1101, CA
p-p53(Ser15)	WB 1:500	Abcam ab1431
p-p53(Ser392)	WB 1:500	CST 9281, Danvers, MA
p21	WB 1:1000, IHC 1:100	CST 2947
p21	IHC 1:100	Abclone A2691, Wuhan, China
Anti- <i>H pylori</i>	IHC 1:200	ZSGB-BIO ZA-0127, Beijing, China
CagA	WB 1:500	GeneTex GTX42382, CA
BrdU	Immunofluorescence (IF) 1:250	Abcam ab6326
CXCR2	WB 1:500	Abcam ab65968
CXCR2	IHC 1:100	Abcam ab14935
Cxcl1	IHC 1:100	Santa Cruz sc-365870, CA
$\beta$ -tubulin	WB 1:1000	CST 2128
$\gamma$ H2AX	IHC 1:100	Abcam ab26350
GAPDH	WB 1:2000	JETWAY SF-PA005, Guangzhou, China
IKK	WB 1:1000	CST 8943
pIKK	WB 1:1000	CST 2697
IKB $\alpha$	WB 1:1000	CST 4814
pIKB $\alpha$ (Ser32)	WB 1:1000	CST 2859
RELA	WB 1:1000	CST 8242
p-RELA (Ser536)	WB 1:500	CST 3037
NFKB1	WB 1:1000	CST 13586
STAT1	WB 1:1000	CST 1499
pSTAT1(Tyr701)	WB 1:500	CST 7649
MEF2A	WB 1:2000	Abcam ab76063
CEBPB	WB 1:1000	Abcam ab32358
YY1	WB 1:1000	Abcam ab109228
VDR	WB 1:1000	Abcam ab109234
Erk	WB 1:1000	CST 46953
pErk (Thr202/Tyr204)	WB 1:2000	CST 4370
Cyclin D1	WB 1:1000	CST 2978

The scores for chronic inflammation were as follows: 0, none; 1, some infiltration; 2, mild (few aggregates in submucosa and mucosa); 3, moderate (several aggregates in submucosa and mucosa); 4, marked (many large aggregates in submucosa and mucosa); 5, nearly the entire mucosa contains dense infiltration; and 6, entire mucosa contains dense infiltration.

The scores for atrophy were as follows: 0, none; 1, foci where a few gastric glands are lost or replaced; 2, small areas in which gastric glands have disappeared or been replaced; 3, 25% of gastric glands lost or replaced; 4, 25%–50% of gastric glands lost or replaced; 5, 50% of gastric glands lost or replaced; and 6, only a few small areas of gastric differentiated glands remaining.

The scores for intestinal metaplasia were as follows: 0, none; 1, only 1 crypt replaced by intestinal epithelium; 2, 1 focal area (1–4 crypts) replaced; 3, 2 separate foci with metaplasia; 4, multiple foci; 5, 50% of gastric epithelium replaced by metaplasia; and 6, only a few small areas of gastric epithelium were not replaced by intestinal epithelium.

For dysplasia, the scores were as follows: 0, none; 1, only 1 crypt replaced by dysplasia; 2, 1 focal area (1–4 crypts) replaced; 3, 2 separate foci with dysplasia; 4, multiple foci;

**Table 3.** Primers Used in ChIP

Gene	Primer sequence
ChIP- <i>NFKB1</i> -RE1	Forward
	Reverse
ChIP- <i>NFKB1</i> -RE2	Forward
	Reverse
ChIP- <i>NFKB1</i> -RE3	Forward
	Reverse
ChIP- <i>TP53</i> -RE1	Forward
	Reverse
ChIP- <i>TP53</i> -RE2	Forward
	Reverse

**Table 4.** Primers Used for Quantitative Real-Time PCR

Gene (protein name)	Primer sequence
<i>CXCR2</i> (CXCR2)	
Forward	CCTGTCTTACTTTTCCGAAGGAC
Reverse	TTGCTGTATTGTTGCCATGT
<i>CXCL1</i> (CXCL1)	
Forward	ATTCACCCCAAGAACATCCA
Reverse	GATGCAGGATTGAGGCAAG
<i>CXCL8</i> (CXCL8)	
Forward	ACTGAGAGTGATTGAGAGTGGAC
Reverse	AACCCTCTGCACCCAGTTTTC
<i>TP53</i> (p53)	
Forward	GAGGTTGGCTCTGACTGTACC
Reverse	TCCGTCCAGTAGATTACCAC
<i>CDKN1A</i> (p21)	
Forward	TGTCCGTCAGAACCCATGC
Reverse	AAAGTCGAAGTTCATCGCTC
<i>CDKN2A</i> (p16)	
Forward	ATGGAGCCTTCGGCTGACT
Reverse	GTAACTATTCGGTGC GTTGGG
<i>CDKN1B</i> (p27)	
Forward	ATCACAACCCCTAGAGGGCA
Reverse	GGGTCTGTAGTAGAACTCGGG
<i>RB1</i> (Rb)	
Forward	CACCTTTGTGAACGCCTTCTGT
Reverse	CACGTTTGAATGTCTCCTGAACA
<i>GAPDH</i> (GAPDH)	
Forward	ACAACCTTGGTATCGTGGAAGG
Reverse	GCCATCACGCCACAGTTTC
<i>Cxcr2</i> (Cxcr2)	
Forward	ATGCCCTCTATTCTGCCAGAT
Reverse	GTGCTCCGGTTGTATAAGATGAC
<i>Cxcl1</i> (Cxcl1)	
Forward	CTGGGATTCACCTCAAGAACATC
Reverse	CAGGGTCAAGGCAAGCCTC
<i>Gapdh</i> (Gapdh)	
Forward	GAACGGGAAGCTCACTGG
Reverse	GCCTGCTTCACCACCTTCT

5, 50% of gastric epithelium replaced by dysplasia; and 6, only a few small areas of gastric epithelium were not replaced by dysplasia.

The scores for neutrophil infiltration were as follows: 0, none; 1, some infiltrates; 2, mild (few aggregates in submucosa and mucosa); 3, moderate (several aggregates in submucosa and mucosa); 4, marked (many large aggregates in submucosa and mucosa); 5, nearly the entire mucosa contains a dense infiltrate; and 6, entire mucosa contains a dense infiltrate.

### *H. pylori* Colonization Analysis in Mouse Mucosa Samples

The histologic score of *H. pylori* colonization was analyzed according to a previous study.<sup>52</sup>

### Western Blot

For Western blot analysis, total proteins from cell lines and fresh-frozen tissues were extracted using the Whole Cell Protein Extraction Kit (KeyGEN BioTECH, Wuhan,

China). A BCA Protein Quantitation Assay (KeyGEN BioTECH) was used to measure the protein concentration. An equal amount (30  $\mu$ g) of protein sample was separated on 10% sodium dodecyl sulfate-polyacrylamide gels and transferred to polyvinylidene fluoride membranes (Millipore, MA). The membranes then were blocked with 5% nonfat dry milk in Tris-buffered saline/0.1% Tween 20 for 1 hour at room temperature. The membranes were incubated with appropriate primary antibodies (Table 3) overnight at 4°C. The next day, the membranes were washed and incubated with horseradish-peroxidase-conjugated secondary antibody. Proteins were visualized using Immobilon Western Chemiluminescent Horseradish-Peroxidase Substrate (Millipore).

### Luciferase Reporter Assay

The wild-type and mutated promoter regions of CXCR2 were subcloned into the pGL4.1 reporter (pCXCR2-luci). The luciferase assay kit was obtained from GeneCopoeia, and the experiments were performed according to the manufacturer's instructions. To examine whether the transcriptional activity of CXCR2 was regulated by RELA, NFKB1, or exogenous wild-type p53, the 293T or AGS cells ( $2 \times 10^4$ ) were seeded the day before transfection into 48-well plates. Next, 200 ng pCXCR2-luci, 10 ng pRenilla reporter, and the corresponding plasmid were co-transfected into cells with Lipofectamine 3000 reagent (Invitrogen). After transfection (48 h), cells were harvested and prepared for luciferase activity analysis according to the manufacturer's instructions. To explore whether CXCR2 transcriptional activity was regulated by endogenous wild-type p53 or *H. pylori*, AGS cells ( $4 \times 10^4$ ) were seeded the day before transfection into 48-well plates. Next, 200 ng pCXCR2-luci and 10 ng pRenilla reporter were cotransfected with Lipofectamine 3000 reagent. After transfection (24 h), the cell culture medium was replaced with fresh media containing Nutlin3 (10  $\mu$ mol/L) or *H. pylori* 12 hours later, the cells were harvested, and luciferase activity was measured.

### ChIP

For ChIP analysis,  $2 \times 10^7$  AGS cells were stimulated with IL1 $\beta$  for 30 minutes (8 ng/mL; R&D Systems, MN) or Nutlin3 for 12 hours (10  $\mu$ mol/L; Selleck, Shanghai, China) and then harvested for experiments according to the manufacturer's instructions in the ChIP Kit (17-10086; Millipore). In brief, 10  $\mu$ L primary anti-NFKB1 antibody and 5  $\mu$ L primary anti-p53 antibody were used for each reaction. Anti-RNA polymerase II antibody was used as a positive control, and IgG was used as the negative control. Purified DNA was analyzed using qPCR to calculate the fold change in enrichment or with standard end point PCR followed by 2% agarose gel electrophoresis. The primers used are listed in Table 4.

### GEO Data Analysis and Transcription Factor Prediction

The GEO series used in this study, namely, GSE47797, GSE3556, and GSE65458, were downloaded from GEO data

sets (<https://www.ncbi.nlm.nih.gov/gds>). Cut-off values of analyses using the GEO series are indicated in the Figure legends (Figure 5A). Data were analyzed using GSEA. Transcription factor prediction was performed using PROMO ([http://algggen.lsi.upc.es/cgi-bin/promo\\_v3/promo/promoinit.cgi?dirDB=TF\\_8.3](http://algggen.lsi.upc.es/cgi-bin/promo_v3/promo/promoinit.cgi?dirDB=TF_8.3)) and JASPAR (<http://jaspardev.genereg.net>) software. Factors predicted in PROMO with a dissimilarity margin of 15% or less were chosen for analysis. A threshold of 80% was used in JASPAR.

### Cell Senescence Model Induced by DNA Damage

To induce the in vitro cell senescence model,  $1 \times 10^5$  cells were seeded in a 12-well plate, and after 24 hours the cells were exposed to 3–10 Gy X-ray (RS2000; Rad Source Technologies, GA). After culturing for another 3–5 days, the cells were prepared for further experiments, including Western blot analysis, qPCR, SA- $\beta$ -gal staining, and BrdU analyses.

### Animal Model

Six-week-old female C57BL6/J mice were used according to previous studies,<sup>53,54</sup> obtained from the Model Animal Research Center of Nanjing University (Nanjing, China) and housed under specific pathogen-free conditions with 12-hour dark/light cycles and free access to water and food. Mice were housed in microisolator static cages with autoclaved nesting materials and hardwood bedding. Animals were inoculated with the *H pylori* strain PMSS1 with or without MNU according to a previous study.<sup>54</sup> All animal experimental procedures were approved by the Institutional Ethical Committee of the First Affiliated Hospital of Sun Yat-sen University and performed in accordance with the National Institutes of Health guidelines for the care and use of laboratory animals. The first animal experiment contained 2 groups: the control ( $n = 5$ ) and PMSS1-infected groups ( $n = 12$ ). The mice were inoculated with *H pylori* ( $1 \times 10^9$  CFU/mL) every other day 3 times at 6 weeks of age. Another animal experiment contained 6 groups: control, PMSS1 infection only, PMSS1 infection with SB225002 treatment, MNU treatment only, PMSS1 infection with MNU treatment, and PMSS1 infection with MNU and SB225002 treatment. Eighty C57/BL6J mice were divided randomly into these 6 groups: 5 mice were assigned to the control group and 15 mice were assigned to each of the remaining 5 groups. Three mice in the PMSS1 infection group were killed to assess *H pylori* infection at 16 weeks of age. Three mice in the MNU group died during MNU treatment. MNU (200 ppm) was administered to mice in drinking water beginning at 6 weeks of age, replaced twice a week, and protected from light. The mice were inoculated with *H pylori* ( $1 \times 10^9$  CFU/mL) every other day 3 times starting at 18 weeks of age. The mice were killed at 46 weeks of age. SB225002 (Selleck), a selective CXCR2 inhibitor, was given twice a week through intraperitoneal injection until the end of the experiment. The CXCR2 inhibitor (1 mg/kg) was suspended in 1% dimethyl sulfoxide and 0.25% Tween-20 in PBS. Solvent alone was given to the control group. *H pylori* was cultured in Brucella Agar (Hopebio, Shandong,

China) with 5% sheep blood (Ruite Bio, Guangzhou, China). The *H pylori* strain PMSS1 was kindly donated by Professor Liu Side (Nanfeng Hospital, Guangzhou, China) and identified in our laboratory according to a previous study.<sup>55</sup> This strain expresses the key *H pylori* virulence factors vacuolating cytotoxin A and CagA, harbors the type IV secretion system, and can deliver CagA into host cells.

### Access to Data

All authors had access to the study data and reviewed and approved the final manuscript.

### Statistical Analyses

All statistical analyses were performed using GraphPad Prism (version 6.07; GraphPad Prism Software, San Diego, CA) and SPSS (V.23, Chicago, IL). *P* values were calculated using Student *t* tests, chi-square tests, or nonparametric tests. Two-tailed tests and an  $\alpha$  level of .05 were used for all statistical analyses.

### References

- Correa P, Haenszel W, Cuello C, Zavala D, Fontham E, Zarama G, Tannenbaum S, Collazos T, Ruiz B. Gastric precancerous process in a high risk population: cohort follow-up. *Cancer Res* 1990; 50:4737–4740.
- Correa P, Houghton J. Carcinogenesis of Helicobacter pylori. *Gastroenterology* 2007;133:659–672.
- Song H, Ekhedden IG, Zheng Z, Ericsson J, Nyren O, Ye W. Incidence of gastric cancer among patients with gastric precancerous lesions: observational cohort study in a low risk Western population. *BMJ (Clin Res)* 2015;351:h3867.
- Weck MN, Brenner H. Association of Helicobacter pylori infection with chronic atrophic gastritis: meta-analyses according to type of disease definition. *Int J Cancer* 2008;123:874–881.
- Adamu MA, Weck MN, Rothenbacher D, Brenner H. Incidence and risk factors for the development of chronic atrophic gastritis: five year follow-up of a population-based cohort study. *Int J Cancer* 2011; 128:1652–1658.
- Genta RM. Review article: gastric atrophy and atrophic gastritis—nebulous concepts in search of a definition. *Aliment Pharmacol Ther* 1998;12(Suppl 1):17–23.
- Houghton J, Wang TC. Helicobacter pylori and gastric cancer: a new paradigm for inflammation-associated epithelial cancers. *Gastroenterology* 2005; 128:1567–1578.
- Genta RM. Helicobacter pylori, inflammation, mucosal damage, and apoptosis: pathogenesis and definition of gastric atrophy. *Gastroenterology* 1997;113(6 Suppl):S51–S55.
- Genta RM, Graham DY. Comparison of biopsy sites for the histopathologic diagnosis of Helicobacter

- pylori: a topographic study of *H pylori* density and distribution. *Gastrointest Endosc* 1994;40:342–345.
10. Polenghi A, Bossi F, Fischetti F, Durigutto P, Cabrelle A, Tamassia N, Cassatella MA, Montecucco C, Tedesco F, de Bernard M. The neutrophil-activating protein of *Helicobacter pylori* crosses endothelia to promote neutrophil adhesion in vivo. *J Immunol* 2007;178:1312–1320.
  11. Sharpless NE, Sherr CJ. Forging a signature of in vivo senescence. *Nat Rev Cancer* 2015;15:397–408.
  12. Lopez-Otin C, Blasco MA, Partridge L, Serrano M, Kroemer G. The hallmarks of aging. *Cell* 2013;153:1194–1217.
  13. Lasry A, Ben-Neriah Y. Senescence-associated inflammatory responses: aging and cancer perspectives. *Trends Immunol* 2015;36:217–228.
  14. Rodier F, Coppe JP, Patil CK, Hoeijmakers WA, Munoz DP, Raza SR, Freund A, Campeau E, Davalos AR, Campisi J. Persistent DNA damage signalling triggers senescence-associated inflammatory cytokine secretion. *Nat Cell Biol* 2009;11:973–979.
  15. Krtolica A, Parrinello S, Lockett S, Desprez PY, Campisi J. Senescent fibroblasts promote epithelial cell growth and tumorigenesis: a link between cancer and aging. *Proc Natl Acad Sci U S A* 2001;98:12072–12077.
  16. Ohuchida K, Mizumoto K, Murakami M, Qian LW, Sato N, Nagai E, Matsumoto K, Nakamura T, Tanaka M. Radiation to stromal fibroblasts increases invasiveness of pancreatic cancer cells through tumor-stromal interactions. *Cancer Res* 2004;64:3215–3222.
  17. Bavik C, Coleman I, Dean JP, Knudsen B, Plymate S, Nelson PS. The gene expression program of prostate fibroblast senescence modulates neoplastic epithelial cell proliferation through paracrine mechanisms. *Cancer Res* 2006;66:794–802.
  18. Saito Y, Murata-Kamiya N, Hirayama T, Ohba Y, Hatakeyama M. Conversion of *Helicobacter pylori* CagA from senescence inducer to oncogenic driver through polarity-dependent regulation of p21. *J Exp Med* 2010;207:2157–2174.
  19. Going JJ, Stuart RC, Downie M, Fletcher-Monaghan AJ, Keith WN. 'Senescence-associated' beta-galactosidase activity in the upper gastrointestinal tract. *J Pathol* 2002;196:394–400.
  20. Wang B, Su X, Ke Y. [Activation of proto-oncogenes induced by MNNG on primary culture of human gastric epithelium and immortalized human gastric epithelial cell line] Article in Chinese. *Zhonghua Zhong Liu Za Zhi* 1996;18:6–9.
  21. Olson TS, Ley K. Chemokines and chemokine receptors in leukocyte trafficking. *Am J Physiol Regul Integr Comp Physiol* 2002;283:R7–R28.
  22. Acosta JC, O'Loughlen A, Banito A, Guijarro MV, Augert A, Raguz S, Fumagalli M, Da Costa M, Brown C, Popov N, Takatsu Y, Melamed J, d'Adda di Fagagna F, Bernard D, Hernando E, Gil J. Chemokine signaling via the CXCR2 receptor reinforces senescence. *Cell* 2008;133:1006–1018.
  23. Guo H, Liu Z, Xu B, Hu H, Wei Z, Liu Q, Zhang X, Ding X, Wang Y, Zhao M, Gong Y, Shao C. Chemokine receptor CXCR2 is transactivated by p53 and induces p38-mediated cellular senescence in response to DNA damage. *Aging Cell* 2013;12:1110–1121.
  24. Lesina M, Wormann SM, Morton J, Diakopoulos KN, Korneeva O, Wimmer M, Einwachter H, Sperveslage J, Demir IE, Kehl T, Saur D, Sipos B, Heikenwalder M, Steiner JM, Wang TC, Sansom OJ, Schmid RM, Algul H. RelA regulates CXCL1/CXCR2-dependent oncogene-induced senescence in murine Kras-driven pancreatic carcinogenesis. *J Clin Invest* 2016;126:2919–2932.
  25. Yamaoka Y, Kikuchi S, el-Zimaity HM, Gutierrez O, Osato MS, Graham DY. Importance of *Helicobacter pylori* oipA in clinical presentation, gastric inflammation, and mucosal interleukin 8 production. *Gastroenterology* 2002;123:414–424.
  26. Baik SC, Youn HS, Chung MH, Lee WK, Cho MJ, Ko GH, Park CK, Kasai H, Rhee KH. Increased oxidative DNA damage in *Helicobacter pylori*-infected human gastric mucosa. *Cancer Res* 1996;56:1279–1282.
  27. Sierra JC, Asim M, Verriere TG, Piazuelo MB, Suarez G, Romero-Gallo J, Delgado AG, Wroblewski LE, Barry DP, Peek RM Jr, Gobert AP, Wilson KT. Epidermal growth factor receptor inhibition downregulates *Helicobacter pylori*-induced epithelial inflammatory responses, DNA damage and gastric carcinogenesis. *Gut* 2018;67:1247–1260.
  28. Collado M, Blasco MA, Serrano M. Cellular senescence in cancer and aging. *Cell* 2007;130:223–233.
  29. Bhattacharyya A, Chattopadhyay R, Burnette BR, Cross JV, Mitra S, Ernst PB, Bhakat KK, Crowe SE. Acetylation of apurinic/aprimidinic endonuclease-1 regulates *Helicobacter pylori*-mediated gastric epithelial cell apoptosis. *Gastroenterology* 2009;136:2258–2269.
  30. Wong BC, Lam SK, Wong WM, Chen JS, Zheng TT, Feng RE, Lai KC, Hu WH, Yuen ST, Leung SY, Fong DY, Ho J, Ching CK, Chen JS. *Helicobacter pylori* eradication to prevent gastric cancer in a high-risk region of China: a randomized controlled trial. *JAMA* 2004;291:187–194.
  31. Zhang X, Guo R, Kambara H, Ma F, Luo HR. The role of CXCR2 in acute inflammatory responses and its antagonists as anti-inflammatory therapeutics. *Curr Opin Hematol* 2019;26:28–33.

32. Giroux V, Rustgi AK. Metaplasia: tissue injury adaptation and a precursor to the dysplasia-cancer sequence. *Nat Rev Cancer* 2017;17:594–604.
33. Gao X, Zhang Y, Brenner H. Associations of *Helicobacter pylori* infection and chronic atrophic gastritis with accelerated epigenetic ageing in older adults. *Br J Cancer* 2017;117:1211–1214.
34. Leung WK, Lin SR, Ching JY, To KF, Ng EK, Chan FK, Lau JY, Sung JJ. Factors predicting progression of gastric intestinal metaplasia: results of a randomised trial on *Helicobacter pylori* eradication. *Gut* 2004;53:1244–1249.
35. Mera R, Fonstam ET, Bravo LE, Bravo JC, Piazuelo MB, Camargo MC, Correa P. Long term follow up of patients treated for *Helicobacter pylori* infection. *Gut* 2005;54:1536–1540.
36. You WC, Brown LM, Zhang L, Li JY, Jin ML, Chang YS, Ma JL, Pan KF, Liu WD, Hu Y, Crystal-Mansour S, Pee D, Blot WJ, Fraumeni JF Jr, Xu GW, Gail MH. Randomized double-blind factorial trial of three treatments to reduce the prevalence of pre-cancerous gastric lesions. *J Natl Cancer Inst* 2006;98:974–983.
37. Shiao YH, Rugge M, Correa P, Lehmann HP, Scheer WD. p53 alteration in gastric precancerous lesions. *Am J Pathol* 1994;144:511–517.
38. Deguchi R, Takagi A, Kawata H, Inoko H, Miwa T. Association between CagA+ *Helicobacter pylori* infection and p53, bax and transforming growth factor-beta-RII gene mutations in gastric cancer patients. *Int J Cancer* 2001;91:481–485.
39. Shibata A, Parsonnet J, Longacre TA, Garcia MI, Puligandla B, Davis RE, Vogelmann JH, Orentreich N, Habel LA. CagA status of *Helicobacter pylori* infection and p53 gene mutations in gastric adenocarcinoma. *Carcinogenesis* 2002;23:419–424.
40. Toller IM, Neelsen KJ, Steger M, Hartung ML, Hottiger MO, Stucki M, Kalali B, Gerhard M, Sartori AA, Lopes M, Muller A. Carcinogenic bacterial pathogen *Helicobacter pylori* triggers DNA double-strand breaks and a DNA damage response in its host cells. *Proc Natl Acad Sci U S A* 2011;108:14944–14949.
41. Matsumoto Y, Marusawa H, Kinoshita K, Endo Y, Kou T, Morisawa T, Azuma T, Okazaki IM, Honjo T, Chiba T. *Helicobacter pylori* infection triggers aberrant expression of activation-induced cytidine deaminase in gastric epithelium. *Nat Med* 2007;13:470–476.
42. Derks S, Bass AJ. Mutational signatures in *Helicobacter pylori*-induced gastric cancer: lessons from new sequencing technologies. *Gastroenterology* 2014;147:267–269.
43. Slack JM. Metaplasia and transdifferentiation: from pure biology to the clinic. *Nat Rev Mol Cell Biol* 2007;8:369–378.
44. Hayakawa Y, Ariyama H, Stancikova J, Sakitani K, Asfaha S, Renz BW, Dubeykovskaya ZA, Shibata W, Wang H, Westphalen CB, Chen X, Takemoto Y, Kim W, Khurana SS, Taylor Y, Nagar K, Tomita H, Hara A, Sepulveda AR, Setlik W, Gershon MD, Saha S, Ding L, Shen Z, Fox JG, Friedman RA, Konieczny SF, Worthley DL, Korinek V, Wang TC. Mist1 expressing gastric stem cells maintain the normal and neoplastic gastric epithelium and are supported by a perivascular stem cell niche. *Cancer Cell* 2015;28:800–814.
45. Mills JC, Goldenring JR. Metaplasia in the stomach arises from gastric chief cells. *Cell Mol Gastroenterol Hepatol* 2017;4:85–88.
46. Kalisperati P, Spanou E, Pateras IS, Korkolopoulou P, Varvarigou A, Karavokyros I, Gorgoulis VG, Vlachoyiannopoulos PG, Sougioultzis S. Inflammation, DNA damage, *Helicobacter pylori* and gastric tumorigenesis. *Front Genet* 2017;8:20.
47. Con SA, Takeuchi H, Valerin AL, Con-Wong R, Con-Chin GR, Con-Chin VG, Nishioka M, Mena F, Brenes F, Yasuda N, Araki K, Sugiura T. Diversity of *Helicobacter pylori* cagA and vacA genes in Costa Rica: its relationship with atrophic gastritis and gastric cancer. *Helicobacter* 2007;12:547–552.
48. Suzuki M, Mimuro H, Kiga K, Fukumatsu M, Ishijima N, Morikawa H, Nagai S, Koyasu S, Gilman RH, Kersulyte D, Berg DE, Sasakawa C. *Helicobacter pylori* CagA phosphorylation-independent function in epithelial proliferation and inflammation. *Cell Host Microbe* 2009;5:23–34.
49. Evangelou K, Gorgoulis VG. Sudan Black B, the specific histochemical stain for lipofuscin: a novel method to detect senescent cells. *Methods Mol Biol* 2017;1534:111–119.
50. Detre S, Saclani Jotti G, Dowsett M. A "quickscore" method for immunohistochemical semiquantitation: validation for oestrogen receptor in breast carcinomas. *J Clin Pathol* 1995;48:876–878.
51. Sayi A, Kohler E, Hitzler I, Arnold I, Schwendener R, Rehrauer H, Muller A. The CD4+ T cell-mediated IFN-gamma response to *Helicobacter* infection is essential for clearance and determines gastric cancer risk. *J Immunol* 2009;182:7085–7101.
52. Lee A, O'Rourke J, De Ungria MC, Robertson B, Daskalopoulos G, Dixon MF. A standardized mouse model of *Helicobacter pylori* infection: introducing the Sydney strain. *Gastroenterology* 1997;112:1386–1397.
53. Sutton P, Danon SJ, Walker M, Thompson LJ, Wilson J, Kosaka T, Lee A. Post-immunisation gastritis and *Helicobacter* infection in the mouse: a long term study. *Gut* 2001;49:467–473.
54. Hahm KB, Kim DH, Lee KM, Lee JS, Surh YJ, Kim YB, Yoo BM, Kim JH, Joo HJ, Cho YK, Nam KT, Cho SW. Effect of long-term administration of rebamipide on

[Helicobacter pylori infection in mice. Aliment Pharmacol Ther 2003;18\(Suppl 1\):24–38.](#)

55. Draper JL, Hansen LM, Bernick DL, Abedrabbo S, Underwood JG, Kong N, Huang BC, Weis AM, Weimer BC. Fallacy of the unique genome: sequence diversity within single *Helicobacter pylori* strains. [mBio 2017;8:e02321.](#)

---

Received January 16, 2020. Accepted October 29, 2020.

#### Correspondence

Center of Gastrointestinal Surgery, First Affiliated Hospital, Sun Yat-sen University, No. 58 Zhongshan 2nd Road Guangzhou, Guangdong Province, PR China 510080. e-mail: [xjianb@mail.sysu.edu.cn](mailto:xjianb@mail.sysu.edu.cn); [heyulong@mail.sysu.edu.cn](mailto:heyulong@mail.sysu.edu.cn); fax: (86) 20-28823389.

#### CRediT Authorship Contributions

Qinbo Cai (Data curation: Lead; Formal analysis: Lead; Investigation: Lead; Methodology: Lead; Writing – original draft: Lead);

Peng Shi (Data curation: Supporting; Formal analysis: Supporting; Investigation: Supporting; Methodology: Supporting);  
Yujie Yuan (Data curation: Supporting; Investigation: Supporting);  
Jianjun Peng (Data curation: Supporting; Formal analysis: Supporting);  
Xinde Ou (Data curation: Supporting; Investigation: Supporting);  
Wen Zhou (Formal analysis: Supporting; Methodology: Supporting);  
Jin Li (Data curation: Supporting; Investigation: Supporting);  
Taiqiang Su (Data curation: Supporting; Investigation: Supporting);  
Liangliang Lin (Data curation: Supporting; Investigation: Supporting);  
Shirong Cai (Validation: Supporting; Writing – review & editing: Supporting);  
Yulong He (Funding acquisition: Lead; Project administration: Lead; Writing – review & editing: Lead);  
Jianbo Xu, Ph.D., M.D. (Funding acquisition: Lead; Project administration: Lead; Supervision: Lead; Writing – review & editing: Lead).

#### Conflicts of interest

The authors disclose no conflicts.

#### Funding

This study was supported by the National Natural Foundation of China (81472260, 81672343, and 81871915 to J.B.X.; 81772579 to Y.L.H.), Natural Science Foundation of Guangdong, China (2015A030313053 and 2017A030313570 to J.B.X.; 2016A020213002 to Y.L.H.), Science and Technology Program of Guangzhou, China (201510010146 to Y.L.H.; 201607010050 to J.B.X.), and The Fundamental Research Funds for the Central Universities (15ykpy17 to J.B.X.).